Remote Sensing of Environment 316 (2025) 114507

Contents lists available at ScienceDirect

Remote Sensing of Environment

journal homepage: www.elsevier.com/locate/rse

Evaluating the utility of hyperspectral data to monitor local-scale β-diversity across space and time

Joseph J. Everest [a,*], Elisa Van Cleemput [b,c,d], Alison L. Beamish [e], Marko J. Spasojevic [f], Hope C. Humphries [c], Sarah C. Elmendorf [b,c]

[a] School of GeoSciences, The University of Edinburgh, 401 Crew Building, The King's Buildings, West Mains Road, Edinburgh, EH9 3FF, United Kingdom
[b] Department of Ecology and Evolutionary Biology, University of Colorado Boulder, 1900 Pleasant Street, 334 UCB, Boulder, CO 80309, United States of America
[c] Institute of Arctic and Alpine Research, University of Colorado, Campus Box 450, Boulder, CO 80309-0450, United States of America
[d] Leiden University College The Hague, Leiden University, Anna van Buerenplein 301, 2595, DG Den Haag, the Netherlands
[e] Department of Geodesy, Section of Remote Sensing and Geoinformatics Helmholtz Centre Potsdam – German Centre for Geosciences (GFZ), Germany
[f] Department of Evolution, Ecology, and Organismal Biology, University of California Riverside, Riverside, CA 92521, United States of America

ARTICLE INFO

Edited by: Jing M. Chen

Keywords:
Functional traits
Hyperspectral
Remote sensing
Beta-diversity
Functional diversity
Species diversity
NEON
Biomass
NDVI

ABSTRACT

Plant functional traits are key drivers of ecosystem processes. However, plot-based monitoring of functional composition across both large spatial and temporal extents is a time-consuming and expensive undertaking. Airborne and satellite remote sensing platforms collect data across large spatial expanses, often repeatedly over time, raising the tantalising prospect of detection of biodiversity change over space and time through remotely sensed methods. Here, we test the degree to which in situ measurements of taxonomic and functional β-diversity, defined as pairwise dissimilarity either between sites, or between years within individual sites, is detectable in airborne hyperspectral imagery across both space and time in an alpine vascular plant community in the Front Range, Colorado, USA. Functional and taxonomic dissimilarity were significantly related to spectral dissimilarity across space, but lacked robust relationships with spectral dissimilarity over time. Biomass showed stronger relationships with spectral dissimilarity than either taxonomic or functional dissimilarity over space, but exhibited no significant associations with spectral dissimilarity over time. Comparative analyses using NDVI revealed that NDVI alone explains much of the variation explained by the full-range spectra. Our results support the use of hyperspectral data to detect fine-scale changes in vascular plant β-diversity over space, but suggest that methodological limitations still preclude the use of this technology for long-term monitoring and change detection.

1. Introduction

Plant functional traits are a primary determinant of ecosystem services ranging from soil fertility levels to water availability and climate feedbacks (Díaz and Cabido, 2001; Häger and Avalos, 2017; Lavorel et al., 2007; Miedema Brown and Anand, 2022; Ottoy et al., 2017; Wang et al., 2019; Zylstra et al., 2016). Shifts in the functional traits – the suite of biochemical, physiological and structural characteristics that affect the uptake and use of resources (Jetz et al., 2016) – of plant communities are therefore likely to have cascading effects on fundamental ecosystem services on which communities – floral, faunal, human or otherwise – rely (Imbert et al., 2021). Changes in the abundances of species with particular traits may provide an early indicator of future tipping points in ecosystem service provisioning (Schweiger and Laliberté, 2022; Villéger et al., 2013). As such, detecting changes in plant community functional composition is a critical component of biodiversity monitoring.

One method for detecting important changes in ecosystem services is by tracking β-diversity, a suite of metrics that quantify the dissimilarity in species and more recently functions across communities over space and time (Anderson et al., 2011; Bishop et al., 2015). β-diversity (change in community structure) can be quantified as simply variation among sites or along pre-defined environmental gradients; here we employ the former definition. A recent synthesis of biodiversity change emphasized that species replacement – not change in species richness – is the dominant form of global biodiversity change seen in long-term

* Corresponding author.
E-mail address: joseph.j.everest@gmail.com (J.J. Everest).

https://doi.org/10.1016/j.rse.2024.114507
Received 8 February 2024; Received in revised form 31 October 2024; Accepted 4 November 2024
Available online 13 November 2024

monitoring studies (Blowes et al., 2019). However, given the time-consuming and costly nature of the on-the-ground sampling needed for longitudinal monitoring of taxonomic β-diversity, the geographic extent of rapid changes in community composition remains unknown. Assessing whether widespread changes in functional β-diversity are also occurring is similarly challenging due to the costs associated with in-situ sampling of traits over spatial domains beyond the local-scale and/or extended time periods (Serbin and Townsend, 2020).

Remote sensing offers the possibility of enhanced characterisation of vegetation diversity by providing repeat, consistent measurements across large, often under sampled spatial extents (Anderson, 2018; Wang et al., 2022). This application requires spatially extensive time series of imagery with sufficient spectral resolution and range to detect change on the ground (Wang and Gamon, 2019). There is a trade-off between the spatial, temporal and spectral resolution of most remote sensing datasets currently available (Gamon et al., 2019; Turner, 2014), but scheduled satellite campaigns seek to fill this gap. For example, the CHIME hyperspectral satellite (European Space Agency, 2023a) will provide global-scale hyperspectral imagery at regular intervals, whilst NASA's ABoVE and NEON's AOP missions have provided high resolution airborne hyperspectral imagery with typically annual repeats over large areas (Miller et al., 2019; NEON, 2023a). Both the continued collection of spatially and temporally consistent hyperspectral data and its assessment against in situ field data are required to determine the feasibility of using remotely sensed hyperspectral data in global biodiversity assessment and monitoring. A coupled approach that leverages field data to provide context and real-world validation for remotely sensed data may prove to be the most effective method to monitor biodiversity at the global scale (Baldeck and Asner, 2013; Gholizadeh et al., 2019; Gillespie et al., 2008; Turner et al., 2003).

Spectra have been used to characterise multiple aspects of terrestrial vegetation diversity, including taxonomic, phylogenetic and functional diversity (Rossi et al., 2022; Schweiger et al., 2018; Stasinski et al., 2021; Wang et al., 2022; Wang et al., 2018). Plots with high spectral diversity typically exhibit high species richness (taxonomic α-diversity) (Carlson et al., 2007; Gholizadeh et al., 2019; Kishore et al., 2023; Marzialetti et al., 2021; Rocchini, 2007; Van Cleemput et al., 2023; Wang et al., 2018). However, it is ultimately not taxonomy per se, but rather variation in physiological and structural traits that determine a plant's optical properties (Gholizadeh et al., 2019; Serbin and Townsend, 2020; Ustin and Gamon, 2010; Wang et al., 2022; Wang et al., 2018). Imaging spectroscopy has long been known to accurately characterise physical and biochemical properties of key ecological processes (Gamon et al., 2023; Haboudane et al., 2004; Tagliabue et al., 2019; Ustin et al., 2004; Zarco-Tejada et al., 2001). As a result, spectral signatures typically reflect the particular ecosystem functions plants provide (hereafter plant functional traits) (Dahlin et al., 2013; Homolová et al., 2013; Meng et al., 2019; Schneider et al., 2017; Suding et al., 2008; Thomson et al., 2021; Wang et al., 2019) and likely track functional composition more strongly than taxonomic composition (Serbin and Townsend, 2020).

A growing corpus of research has investigated the relationship between spectral diversity and plant functional diversity (Beccari et al., 2024; Schneider et al., 2017; Schweiger et al., 2018). Most studies to date have focused on the local scale (α-diversity) component of functional diversity, with very few assessing plant functional β-diversity components (Asner et al., 2017). In contrast there are numerous examples of tracking taxonomic β-diversity (changes in species composition) across space with hyperspectral data (Baldeck and Asner, 2013; Féret and Asner, 2014; Féret and De Boissieu, 2020; Laliberté et al., 2020; Rocchini et al., 2018). It has been argued that tracking changes in plant functional traits *through time* on globally relevant scales can be achieved only through hyperspectral time series due to the cost-prohibitive nature of field campaigns (Jetz et al., 2016). The strong connections between optical properties and plant functional traits also suggest that detecting functional turnover over time may in fact be easier than detecting species turnover.

Despite this strong theoretical grounding, we are not currently aware of any studies investigating the value of hyperspectral imagery in detecting functional β-diversity over time. One reason for the absence of such studies is likely limitations in the availability of comparable spectral time series data (Gamon et al., 2019). Other technical issues may also make the application of hyperspectral remote sensing data to detect functional β-diversity over time challenging. Plant traits, and hence optical properties, evolve asynchronistically throughout and between growing seasons (Gamon et al., 2020; Gholizadeh et al., 2020; Gholizadeh et al., 2019; Rossi et al., 2022; Serbin and Townsend, 2020; Wang et al., 2022; Yang et al., 2016). As a result, disentangling long-term change in vegetation function from intra-annual variability may prove difficult. Multisite airborne campaigns generally face a host of challenges related to cost, instrument and personnel availability and weather conditions which can lead to inconsistency in revisit periods (e.g. Musinsky et al., 2022). This inconsistency in timing can reduce the comparability of multi-year hyperspectral time series and prove challenging for detection of functional diversity over time (Rocchini et al., 2018).

Whilst spectral studies of the vegetation diversity have been carried out in numerous settings, alpine tundra ecosystems typically remain less well represented in hyperspectral studies compared to other key biomes (Gholizadeh et al., 2019; Van Cleemput et al., 2023). This is likely due to the fine-scale compositional and functional heterogeneity that typically characterises tundra communities (Nelson et al., 2022; Rossi et al., 2022; Yang et al., 2020). It is also likely a result of the inherent issues of inaccessibility, cloud cover and extreme weather that working in such environments as the tundra encompass.

Here, we evaluate the capacity of airborne hyperspectral imagery to monitor fine-scale vascular plant functional β-diversity, in alpine tundra vegetation, over both space and time, specifically inter-annually. We define β-diversity as pairwise dissimilarity between sites, or between years for individual sites, in either taxonomic, functional, or spectral dimensions (Anderson et al., 2011; Bishop et al., 2015). We will ask three main questions: 1) is spectral dissimilarity indicative of fine-scale functional variation across space and/or time; 2) does spectral dissimilarity most closely track in situ dissimilarity in functional composition, taxonomic composition, or biomass (an exemplar ecosystem function frequently targeted in remote sensing campaigns); and 3) do simpler, derived spectral products, namely the normalized difference vegetation index (NDVI), predict such dissimilarity similarly well to full-range spectra?

2. Materials & methods

2.1. Study area

The study area, henceforth termed the 'Saddle', is located in a depression between two knolls on Niwot Ridge, in the Indian Peaks Wilderness of the Colorado Front Range, USA (Fig. 1). It comprises a grid of 88 1 m^2 long-term monitoring plots, each grouped into one of eight vegetation classes (Fig. 1) (Spasojevic et al., 2013). The site is monitored as part of the Niwot Ridge Long-term Ecological Research Program (Niwot Ridge LTER, 2023). The plots are located within an area ~550 × 450 m in size (40.06°N, −105.59°E) and range in elevation from 3510 to 3570 m a.s.l. (Fig. 1) (NEON, 2023b). The area comprises entirely alpine tundra and experiences relative climatic extremes annually. The site is predominantly snow covered between the months of December and May and experienced mean summer temperatures of 8.6–9.8 °C between 2017 and 2020 (White et al., 2023).

2.2. Field measurements

Three long-term, in situ monitoring datasets were utilised in this study: 1) plant species composition, 2) above-ground biomass harvests,

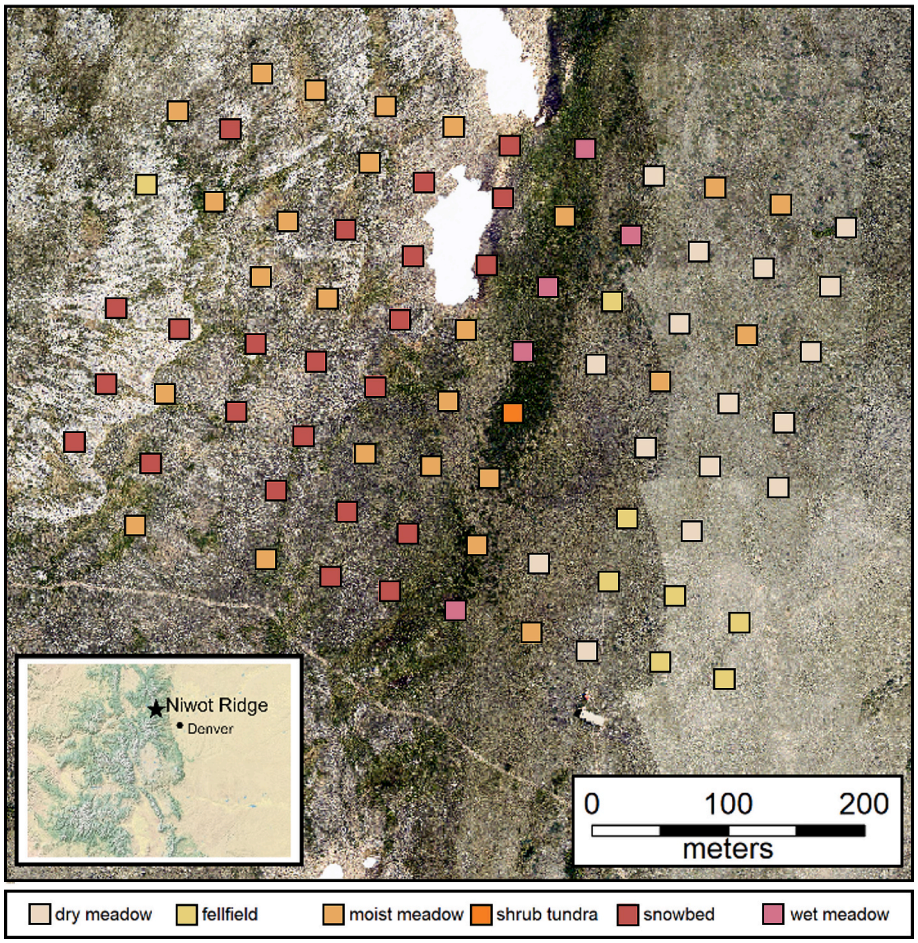

Fig. 1. Study locations on Niwot Ridge. The location of the 78 1 × 1 m^2 assessed plots distributed across the Saddle grid between the East and West Knolls of Niwot Ridge, their corresponding vegetation classes (see legend) and the location of the Niwot Ridge LTER within the Colorado Front Range (see inset). Background imagery is sourced from NEON's high-resolution orthorectified camera imagery mosaic (RGB, 0.1 × 0.1 m resolution) (NEON, 2023c) whilst the inset map is sourced from ESRI © 2014 National Geographic Society, i-cubed.

and 3) plant functional traits. Both composition and biomass data were collected from the 88 Saddle grid plots (Fig. 1). Composition data has been collected throughout the Saddle since 1989, with annual measurements taken since 2010 (Walker et al., 2022a). All occurrences of both living and non-living plant and non-plant material were recorded using 100 pin drops and an 'all-hits' method within the 88 point framing plots. Tundra plant communities typically comprise both canopy and sub-canopy species (Ma et al., 2020) and in order to accurately elucidate community-level dissimilarity, both canopy and sub-canopy species must be accounted for (Ustin and Gamon, 2010). As such, we used an 'all hits' approach. However, whilst field measurements sample both canopy and sub-canopy species, the limited penetration ability of optical remote sensing often prevents the sampling of much of the sub-canopy, particularly in shrub-dominated plots, leading to underrepresentation of sub-canopy individuals and their respective traits within the spectral profile (Ma et al., 2020). As such, we also ran our analyses using a 'top hits' only approach to determine the impact this limited optical penetration had on our ability to characterise community diversity; these results can be seen in Supplementary Materials 1.

Species were taxonomically standardised to the World Flora Online (WFO) Plant List (The Plant List, 2013). Relative cover was then calculated as the percentage of the total hits per plot ascribed to each vascular plant species recorded; non-vascular species were removed due to insufficient ID at the species level. This resulted in a final plot count of 78 (Fig. 1); seven 'barren' plots containing no vascular plant hits were removed, as were two manipulated 'snow fence' plots and one incorrectly geolocated plot. Living vascular plant material comprised 84.9 % of top hits within the retained plots, whilst non-vascular plant material comprised 2.64 %. Plot-level biomass data has been collected since 1992 (Walker et al., 2022b). In each sampling year, a single net primary productivity (NPP) value was measured from a representative area adjacent to each long-term monitoring plot using a combination of clipped biomass and allometry; the latter to prevent damage to sensitive cushion plants. Both datasets were trimmed to the years 2017–2020 to match the hyperspectral imagery availability (Section 2.3). The resulting datasets therefore consisted of 78 plots in each of the four years (316 total), comprising 85 species overall.

Trait records were obtained from samples collected in unmanipulated areas distributed more widely across the Saddle and surrounding tundra at Niwot Ridge during the years 2008–2009, 2017–2018 and 2021 (Spasojevic and Weber, 2008). Traits were sampled predominantly in July and some in August. Whilst our trait data are not temporally aligned with the sampled composition and spectral data, this study benefits from trait measurements being sampled from within the near vicinity of the composition plots at a similar time of year (Fig. 1). In contrast, many trait studies rely on values aggregated across larger spatial and taxonomic scales (Bjorkman et al., 2018; Maitner et al., 2023). Trait values from all measured years were included to maximise the overall size and taxonomic coverage of the dataset. Eight traits – plant height (cm), leaf dry matter content (LDMC; mg g^{-1}), specific leaf area (SLA; cm^2 g^{-1}), δ15N (‰), δ13C (‰), and leaf chlorophyll (μmol m^2), N (%) and C (%) concentrations – were measured following

standard protocols (Perez-Harguindeguy et al., 2016). Each trait relates to the two main axes in plant trait variation - resource acquisition and plant structure (Thomas et al., 2020), is deemed significant to tundra functions and is widely used in tundra trait studies (Bjorkman et al., 2018). Species names were also standardised to the WFO Plant List to allow for the joining of trait values to individual species in the composition records. In total our trait dataset contained 10,303 trait measurements. Trait values were ascribed to individual species via a gap-filling algorithm that generates median trait values – both within vegetation classes and overall – at the species, genus, family and functional group (shrub, forb and graminoid) levels (Supplementary Materials 2). Trait medians were first calculated for each trait within a single species and vegetation class (Fig. 1), then by species alone, then by genus within each vegetation class and so on up to the functional group level, with each species composition record assigned a value for each trait at the lowest taxonomic hierarchy possible. An average of 87.9 % of records were assigned at the species level or lower (Supplementary Materials 2). Plant species together with their traits facilitated the calculation of functional dissimilarity across the Saddle (Section 2.4).

2.3. Hyperspectral imagery

Airborne hyperspectral imagery was sourced from the National Ecological Observatory Network (NEON) 'spectrometer orthorectified surface directional reflectance mosaic' (DP3.30006.001; NEON, 2023a). The level-three processed, 1 × 1 m spatial resolution, 426 band imagery is spectrally calibrated, atmospherically corrected, orthorectified and output onto a uniform 1 × 1 km spatial grid, details of which can be found at Gallery (2022) and Karpowicz and Kampe (2022). The spectra encompass a spectral resolution of 5 nm and range from 380 nm to 2500 nm (NEON, 2023a). Imagery is available across the full study site and is provided as a single mosaic collected between July and August annually from 2017 to 2020 (NEON, 2023a). NEON aims to collect data around the point of peak greenness each assessed year, with data typically collected from flights on three or four days each season. The Saddle (Fig. 1) was typically covered by multiple flightlines on multiple days each season, so reflectance values for individual pixels are selected by NEON from the flightlines with the highest quality cloud conditions and at the closest proximity to nadir (Gallery, 2022). In 2017, 2018 and 2020, all pixels covering the Saddle were selected from the same flightlines during mosaicking, whilst in 2019 pixels were selected from flightlines captured on consecutive days (14th August – 72 plots, 15th August – 6 plots; Fig. 2).

Spectra were extracted from this imagery at the coordinate of each of the 78 retained plots using a circular buffer of 1 m radius; mean spectral reflectances were calculated from all the cells encompassed by each buffer. A 1 m buffer was selected over a 0 m or 3 m buffer to correct for potential geolocation issues in the data (0 m) whilst minimising the risk of inadvertently capturing different vegetation types to that comprising the plot (3 m) (Inamdar et al., 2020); pairwise spectral differences between plots were largely indistinguishable regardless of the buffer selected (R^2: ~0.978–0.988; Supplementary Information 3). Spectral bands both at the spectral extremes (< 400 nm and > 2400 nm) and those that capture atmospheric water (1340–1445 nm and 1790–1995 nm) were then removed (Schweiger and Laliberté, 2022). Broad-band NDVI was calculated from the extracted spectra using wavelengths corresponding to those utilised in the Sentinel-2 10 m bands (band 4: 633–695 nm; band 8: 726–938 nm) (European Space Agency, 2023b). NDVI is an index known to saturate at high biomass levels (Goswami et al., 2015), however due to the relatively low biomass values in this high elevation tundra environment, few plots exceeded the threshold at which NDVI saturation is known to become problematic. To avoid potential artefacts due to shading or exposed soil, specific plots in individual years were removed from analyses based on the plot's respective degree of shading and photosynthetically-active vegetation. A near-infrared (NIR) mask (NIR > 0.2; 752–1048 nm) was employed to remove shaded plots (Rüfenacht et al., 2014; Schweiger and Laliberté, 2022), whilst a NDVI mask (NDVI >0.2; 667 and 827 nm) was utilised to remove plots with limited vegetation cover (Schweiger and Laliberté, 2022).

Further processing steps frequently applied to hyperspectral data include brightness normalization, spectral smoothing and dimensionality reduction. Following the calculation of NDVI and NIR, we brightness normalized our spectra (calculated as the square root of the sum of the reflectances squared) (Feilhauer et al., 2010), but chose not to carry out smoothing or dimensionality reduction. Differences in illumination are known to cause large variations in 'brightness' of plant spectra. Whilst natural differences in brightness are known to be informative of canopy structure (Zhirin et al., 2017), those artificially generated by differences in illumination may obscure the spectral signals of certain leaf traits (Wang et al., 2022). Based on both this and the known influence of illumination differences on both intra-annual and inter-

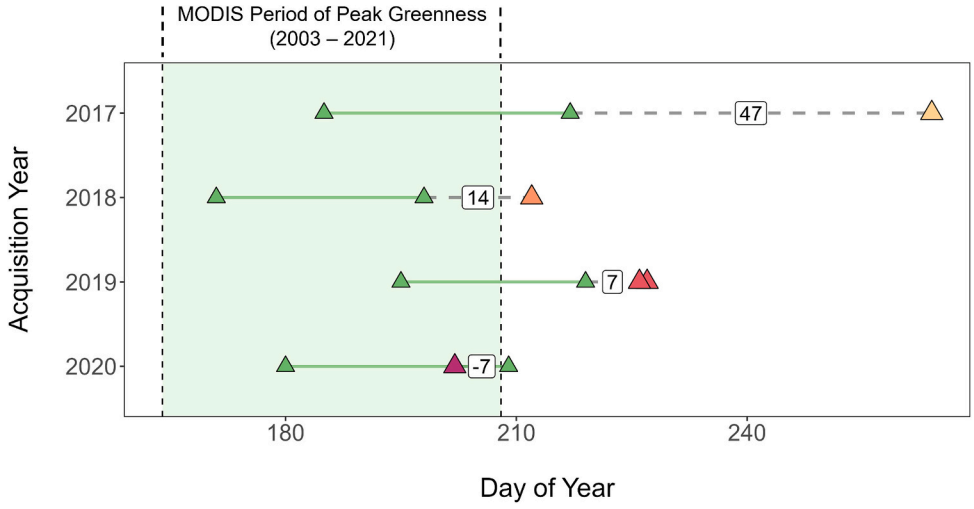

Fig. 2. Timing of hyperspectral data acquisition was generally delayed relative to peak greenness. The coloured triangles represent the day(s) on which the NEON hyperspectral imagery was sampled, the green triangles and lines represent the measured period of peak greenness as measured by NEON's tundra phenocams on Niwot Ridge, with the labelled numbers representing the offset (days delayed) between the end of peak greenness and the date of NEON data acquisition. The green rectangle illustrates the targeted hyperspectral sampling window: mean period of peak greenness between 2003–2021 as measured from MODIS satellite imagery (Musinsky et al., 2022). (For interpretation of the references to colour in this figure legend, the reader is referred to the web version of this article.)

annual hyperspectral data collection, we proceeded with brightness normalization; results both with and without brightness normalization were near identical (Supplementary Materials 4). Smoothing of the resulting spectra, a commonly used method in spectral studies of biodiversity (e.g. Van Cleemput et al., 2023), was also considered to remove random noise (Park et al., 2018), however we declined to undertake this step as it was likely to remove fine-scale, discriminatory features in the spectra. Similarly, dimensionality reduction via principal component analysis (PCA) was also considered, as is standard in many hyperspectral studies given the high-dimensionality of hyperspectral data (e.g. Féret and Asner, 2014). We again declined to undertake this step due to the loss of fine-scale variation and spectral information that occurs in the discarded principal components (Asner et al., 2012). For an example of the resulting spectra in one year, see Supplementary Materials 5.

2.4. β-diversity calculations

Pairwise dissimilarity measures between plot-pairs were calculated for each of the four following metrics – taxonomic composition, functional composition, biomass and spectral composition, (Schweiger and Laliberté, 2022), in order to characterise β-diversity across the Saddle. Methods to calculate β-diversity from remote sensing imagery typically rely on distance-based measures (Rocchini et al., 2018). Different dissimilarity measures were utilised for each variable to ensure the method used was appropriate to the data type. Taxonomic dissimilarity was calculated as abundance-weighted Bray-Curtis dissimilarity, the most commonly used distance metric for species abundance data (Bray and Curtis, 1957; Ricotta and Pavoine, 2022). Functional dissimilarity was calculated as 'functional dissimilarity', or 'FDis' (Ricotta and Pavoine, 2022), a generalised version of their parametric measure aimed at unifying the Euclidean distance and the Bray-Curtis dissimilarity in a manner suitable for use with community composition data. We calculated FDis using median trait values incorporating all years for all eight measured traits as we lacked location- or year-specific values for species traits. As a result, interannual variability in FDis reflects only compositional change and does not incorporate trait plasticity, intraspecific trait variability or seasonal variation in trait expression. Biomass dissimilarity was characterised as the absolute value of the difference between each plot-pair.

Euclidean distance was the selected measure of β-diversity for NDVI and spectral reflectance (Section 2.3). Numerous methods have been used in recent studies to determine 'spectral dissimilarity'. We therefore investigated three separate metrics – 1) Euclidean distance (Chauhan and Krishna Mohan, 2014; Schweiger et al., 2018; Schweiger and Laliberté, 2022), 2) Manhattan distance (Van Cleemput et al., 2019), and 3) Spectral Angle Metric (SAM) (Chauhan and Krishna Mohan, 2014; Van Cleemput et al., 2019) – to determine their respective utility in characterising spectral distance across the Saddle. Upon investigation, it was clear that all of Euclidean distance, Manhattan distance and SAM conformed very closely to one another (Supplementary Materials 6). Euclidean distance between outputted spectra was selected for reasons of both simplicity and consistency.

Pairwise dissimilarity measures were calculated across both space and time. Spatially, dissimilarities were calculated between pairs of plots within individual years (e.g. all plot-pairs in 2017 only), generating 3081 unique plot combinations per year (Supplementary Materials 7). Temporally, distances were calculated for individual plots (e.g. plot 27 only) and between all the pairwise year combinations, generating 6 unique year combinations per plot (Supplementary Materials 8). In doing so, it was possible to facilitate comparisons of dissimilarity in all four assessed variables across the saddle over both space and time. After applying the NDVI & NIR masks (Section 2.3; 11,367 (from a possible 12,324) plot-pair and 453 (from a possible 474) plot-year combinations were retained from the spatial and temporal spectral dissimilarity datasets respectively.

2.5. β-diversity comparisons

In order to determine whether increased spectral dissimilarity is indicative of increased functional dissimilarity, matrices for both functional and spectral dissimilarity were statistically compared using Mantel tests (He and Zhang, 2009; He et al., 2009; Mantel, 1967); spectral matrices were also modelled against taxonomic and biomass distance matrices. Mantel tests were run using the 'Pearson' correlation parameter with 9999 permutations. This method allows for the significance of correlations between pairwise dissimilarity matrices to be assessed whilst accounting for the fact that each plot is included in multiple comparisons (Mantel, 1967). Mantel tests were run between plots within single years for spatial comparisons, and between years for a single plot for temporal comparisons, permuting over all year pair combinations ($n = 6$; Supplementary Materials 7–8). Both R and p-values were obtained from the Mantel tests to determine both the effect size and significance of any given relationship. Given the small number of paired year combinations per plot in the temporal analyses, the statistical power was insufficient to generate meaningful p-values; the calculated R remained sufficient to facilitate between-plot comparisons however. To summarise general patterns in the temporal analyses, mean R values were calculated using the individual R values from the temporal Mantel tests run on each of the 78 plots. Spatial and temporal Mantel tests were also run between NDVI distance matrices and functional, taxonomic and biomass dissimilarity matrices.

3. Results

3.1. Functional ~ spectral dissimilarity relationships

Throughout our study area, functional dissimilarity was positively associated with spectral dissimilarity over space (Fig. 3a) but not time (Fig. 3b). Spatially, the Mantel tests exhibited significant relationships (p: < 0.001–0.002) between functional and spectral dissimilarity within each year, typically with moderate R statistics (R: 0.293–0.555). However, there is little evidence to suggest that plots with substantial functional dissimilarity over time exhibit a greater degree of spectral dissimilarity across the same time period (mean R: 0.106). While we had relatively less power to detect significant relationships across time, with only 4 years of data as compared to 79 plots within each year, the lower R values suggest spectral dissimilarity over time is less strongly related to functional dissimilarity over time than space. A cluster of more functionally dissimilar plot-pairs was evident in all years that reflect the extreme difference in traits between the one shrub-dominated plot in our study area (plot 37) and the remaining, herbaceous-dominated plots (Fig. 3a). Analyses were re-run without plot 37 (Supplementary Materials 9) to ensure that results were robust even without the inclusion of this plot. The direction and significance of all results remained the same between spectral and functional, taxonomic and biomass dissimilarity (Fig. 4a; 4c), with only a small reduction in R values (Supplementary Materials 9). Hence, 'shrubby' plot 37 does exhibit a substantial shift in functions as compared to the non-shrub dominated plots, but was not the primary determinant of the results.

3.2. Taxonomic and biomass ~ spectral dissimilarity relationships

Relationships between taxonomic and spectral dissimilarity were broadly similar to those between functional and spectral dissimilarity (Section 3.1). Over space, when considering taxonomic dissimilarity, the mantel tests again exhibited significant relationships with spectral dissimilarity (p: < 0.001). The strength of the spatial relationships was moderate (R: 0.212–0.384), and tended to be slightly less than the strength of the relationships between functional dissimilarity and spectra (Fig. 4a). Unlike the functional results however, the relationships between taxonomy and spectra over time were similarly strong (mean R: 0.221) to those across space. Whilst the spatial relationships

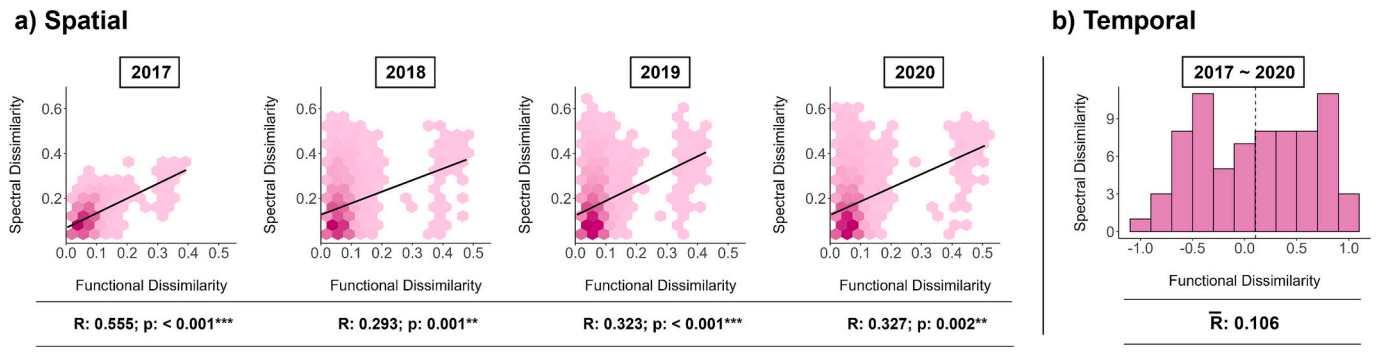

Fig. 3. Pairwise spectral dissimilarity among plots is greater for more functionally dissimilar plots across space but not time. The relationships between functional and spectral dissimilarity: (a) between all plot pairs within each studied year, and (b) for each plot between each pair of study years (e.g. 2017–2018, 2017–2019 and 2017–2020; the dotted line represents the mean dissimilarity). Mantel R and *p* statistics for each year (spatial comparisons only) and averaged over all years (R bar; temporal comparisons only) are provided below the relevant panels (Section 2.5). Linear regression lines are provided as a visual fit of the data.

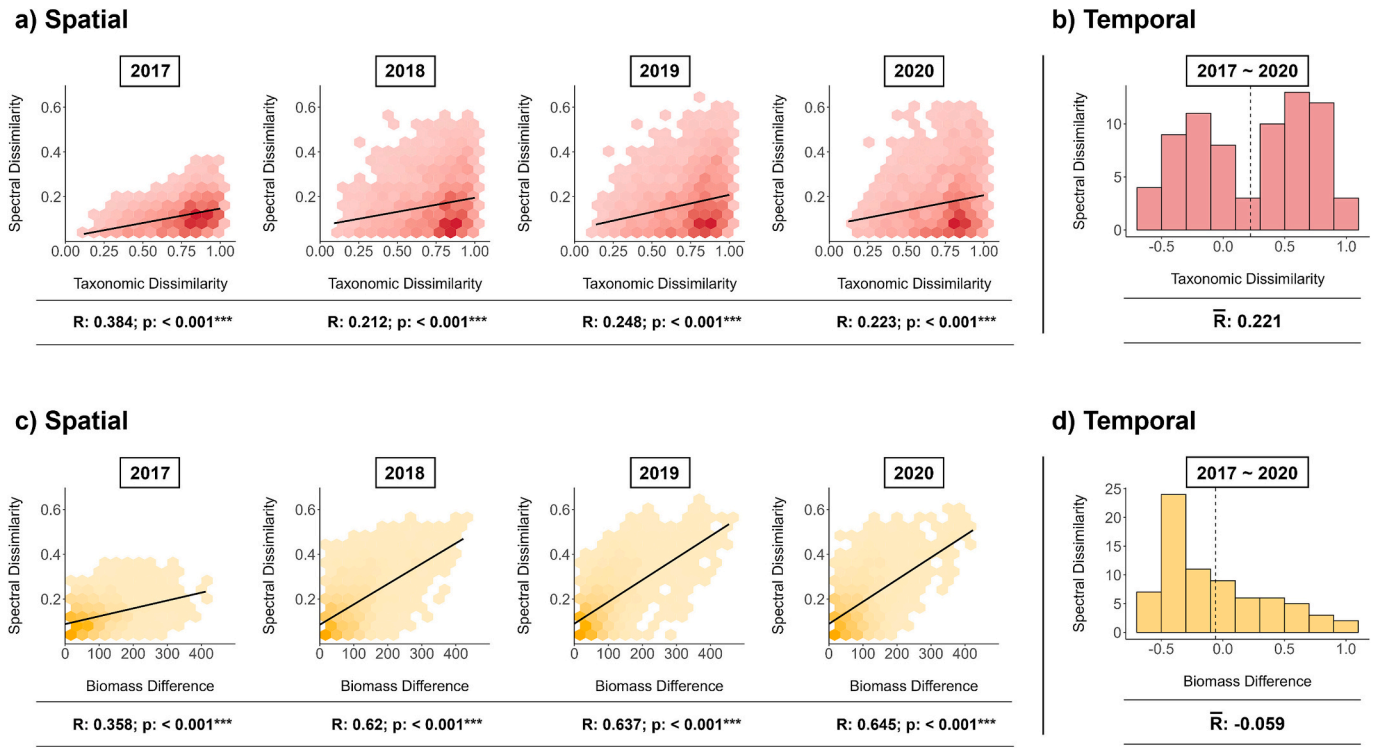

Fig. 4. Pairwise spectral dissimilarity among plots is greater for more taxonomically dissimilar plots and those with greater differences in biomass across space but not time. The relationships between spectral and both taxonomic and biomass dissimilarity: (a, c) between all plot pairs within each studied year, and (b, d) for each plot between each pair of study years (e.g. 2017–2018, 2017–2019 and 2017–2020; the dotted line represents the mean dissimilarity). Mantel R and *p* statistics for each year (spatial comparisons only) and averaged over all years (R bar; temporal comparisons only) are provided below the relevant panels (Section 2.5). Linear regression lines are provided as a visual fit of the data.

were robust to dropping bottom hits, the temporal results largely disappeared when using top hits only (Supplementary Materials 1; mean R: 0.037). As such, we have low confidence in this result. Change in biomass over space was more strongly associated with spectral dissimilarity than either functional or taxonomic dissimilarity. Spatially, biomass is significantly (p: < 0.001) and strongly (R: 0.358–0.648) related to spectral dissimilarity across all years (Fig. 4c), more strongly than either functional or taxonomic dissimilarity (Fig. 3a; 4a). Biomass however conversely exhibited no meaningful relationship over time between in situ and spectral data and displayed the lowest temporal values (mean R: −0.059; Fig. 4d).

3.3. Functional, taxonomic and biomass ~ NDVI relationships

Using NDVI to explain taxonomic, functional and biomass dissimilarity yielded results that were largely similar to those using full spectra (Fig. 5). Mantel tests exhibited significant yet moderate relationships between NDVI and both functional (p: < 0.001–0.002; R: 0.244–0.315) and taxonomic dissimilarity (p: < 0.001; R: 0.215–0.325) across space (Fig. 5a; 5c), with similar patterns also displayed between both metrics and spectral dissimilarity (Fig. 3a; 4a). Again, similarly to spectral dissimilarity, spatial relationships between NDVI and biomass dissimilarity were stronger with NDVI relating significantly and strongly to biomass dissimilarity (p: < 0.001; R: 0.289–0.542; Fig. 5e). Finally, as with full-range spectra, temporal relationships between NDVI dissimilarity and the in situ metrics were weaker to non-existent when

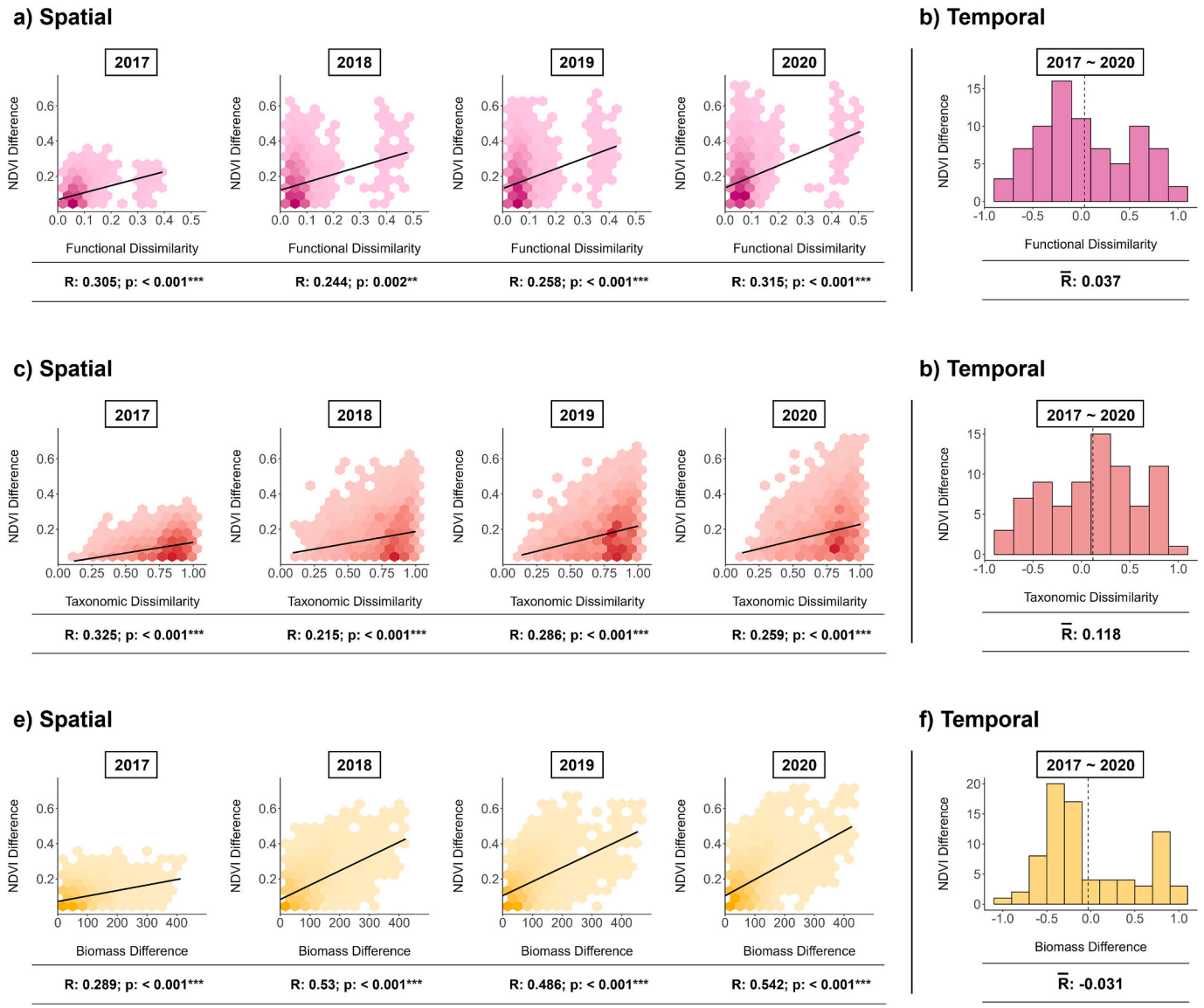

Fig. 5. Functional, taxonomic and biomass dissimilarity among plots track differences in NDVI across space but generally not time. The relationships between NDVI dissimilarity and each of functional (a, b), taxonomic (c, d) and biomass dissimilarity (e, f). Spatial dissimilarity tests relationships between all plot pairs within each studied year, whilst temporal dissimilarity compares relationships for each plot between each pair of study years (e.g. 2017–2018, 2017–2019 and 2017–2020; the dotted line represents the mean dissimilarity). Mantel R and *p* statistics for each year (spatial comparisons only) and averaged over all years (R bar; temporal comparisons only) are provided below the relevant panels (Section 2.5). Linear regression lines are provided as a visual fit of the data.

compared to the spatial ones, with the taxonomic temporal link proving greater than either function or biomass (Figs. 5b; 4b,d). When comparing the strength of the results over space, spectral dissimilarity explains somewhat more variation in both functional and biomass dissimilarity in all years than NDVI dissimilarity, although NDVI dissimilarity in turn explains a greater proportion of the taxonomic dissimilarity between 2018–2020 (Fig. 6).

4. Discussion

4.1. Spectral dissimilarity moderately related to functional β-diversity

Our results highlight the potential utility of using hyperspectral imagery in the detection of fine-scale functional (and taxonomic) β-diversity across space within a single alpine tundra habitat. This supports the much-anticipated promise of using spectral reflectance in functional change detection (Jetz et al., 2016) and the results of other studies that highlighted significant links between spectral reflectance and elements of taxonomic (Baldeck and Asner, 2013; Laliberté et al., 2020; Marzialetti et al., 2021) and functional β-diversity (Asner et al., 2017). Spectral dissimilarity was significantly related to functional and taxonomic dissimilarity across space, although the relationships were only of moderate strength and exhibited considerable scatter (Fig. 3a; 4a). This suggests that whilst both these factors are clearly related, spectral differences are picking up additional factors beyond taxonomic and functional composition. Depending on the intended application, this may be advantageous. For example, our attempts to measure one ecosystem function directly (above-ground biomass) indicated in situ biomass generally showed a stronger spatial association with spectral reflectance than functional dissimilarity did. Relationships between in situ metrics and spectral dissimilarity across years however, were weaker to non-existent. Furthermore, whilst the associated R values suggest a moderately strong relationship between taxonomic and spectral dissimilarity over time, the almost complete removal of that relationship when using top hits only suggests a lack of robustness and reduces the confidence with which we view that result. This may mean that in slow-growing

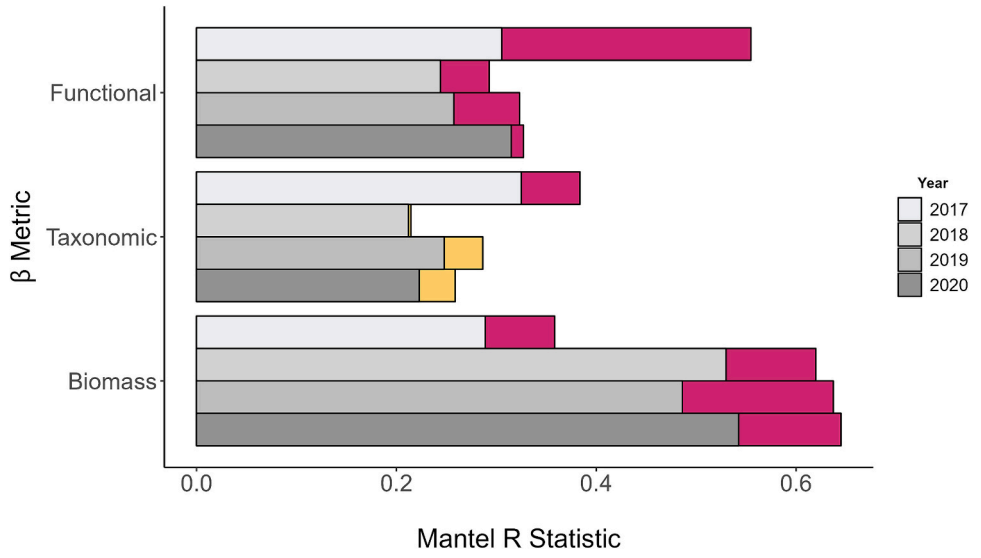

Fig. 6. A substantial proportion of the variation in functional composition, taxonomic composition and biomass among plots explained by hyperspectral dissimilarity can be explained by NDVI alone. Difference in strength of relationship between the three variables and spectral and NDVI dissimilarity respectively; grey bars illustrate the variation explained by both metrics, purple the additional variation explained when using full spectra over NDVI, and orange the additional variation explained when using NDVI over full spectra.

alpine tundra environments, detection of small directional shifts in taxonomic or functional change over time from aerial hyperspectral data may prove difficult, and anticipated promise of monitoring fine-scale β-diversity using spectra alone should be treated with caution (Nelson et al., 2022).

4.2. Why spatial scale matters

Scale issues, over both space and time, likely contribute to the only moderate relationships observed between spectral and functional and taxonomic dissimilarity in this study. Spatially, a core issue comes from the grain size at which comparisons of dissimilarity within the in situ plots and spectral reflectance occur. Past studies have shown that spectral variability best relates to species β-diversity at larger spatial grains. For instance, (Rocchini et al., 2010) found stronger correlations at 20–50 m as opposed to 10 m spatial grains in highland Savannahs. This stems from lower grain sizes typically incorporating higher noise when calculating β-diversity metrics (Rocchini et al., 2010). Past studies often utilise large plots (Laliberté et al., 2020; Rocchini, 2007; Schweiger and Laliberté, 2022; Wang et al., 2016a), although this hinders the fine-scale delineation of vegetation diversity through spectra. The small grain size used in our study (1 × 1 m) reflects the standard plot size for vegetation monitoring in most herbaceous systems. However this grain size may decrease the signal-to-noise ratio and diminishes the strength of relationships between spectral dissimilarity and functional dissimilarity. Smaller spectral pixel sizes, typically 1 mm – 10 cm, are thought to be most appropriate for delineating aspects of fine-scale biodiversity, the size of individual herbaceous plants (Lopatin et al., 2017; Wang et al., 2018). The spectral grain size utilised also precludes the use of a 'spectral species' approach in this study, given that individual tundra plants are typically significantly smaller than the 1 × 1 m grain size, thereby preventing assessments of within-plot dissimilarity and α-diversity through pixel clustering algorithms (Féret and Asner, 2014; Rossi et al., 2022). Where the size of individuals exceeds that of the pixel (e.g., forests, or tundra dominated by large shrubs), such methods may become viable and stronger patterns may emerge as a result. In spite of this, there remains no spatial scale universally considered for the remote detection of biodiversity (Wang et al., 2018).

Spatial mismatches also exist vertically in spectral studies of plant diversity. As outlined in the methods (Section 2.2), whilst field measurements sample both canopy and sub-canopy species, thereby better characterising community function, the limited ability of optical remote sensing to penetrate the canopy results in an underrepresentation of sub-canopy species and their associated traits within each plots' spectral profile (Ma et al., 2020). As such, the spectra may not accurately capture plots' functional composition, weakening relationships between spectral reflectances and in situ estimates of functional dissimilarity and limiting the utility of hyperspectral imagery in such analyses. In our study, on average, 76.5 % of the species found within each plot were present in the canopy layer, with 23.5 % found solely within the sub-canopy layers. When our analyses were re-run with top hits only (Supplementary Materials 1), the strength and significance of the observed relationships between spectral and functional and taxonomic dissimilarity typically remained largely unchanged. This suggests that the hyperspectral imagery is doing a good job of capturing understorey vegetation, possibly because the functional traits of understory plants are similar to those in the canopy. The only result to dramatically change was the taxonomic – spectral relationship across time, which surprisingly reduced in significance when using top hits only; as described above, spectra usually follow top hits better than all hits due to their typical lack of canopy penetration. Moving forwards, if we are to comprehensively and accurately characterise vegetation β-diversity in the future from remotely sensed means, consideration of such factors must continue to be taken into account.

4.3. The importance of timing

Despite evidence for significant spatial relationships between spectral dissimilarity and functional and taxonomic dissimilarity throughout our study system, we found spectral and temporal dissimilarity were typically decoupled from spectral dissimilarity over time. This may stem in large part from the high plasticity, both intra- and inter-annually, displayed by plant traits that can lead to substantial variability in spectral signatures (Osnas et al., 2018; Rossi et al., 2022; Serbin and Townsend, 2020). Alpine tundra ecosystems are characterised by extreme climates and short growing seasons (Nelson et al., 2022), where all plants must progress through leaf development, expansion, flowering and senescence within a few short months. Intraspecific variation due to phenology may exceed interspecific variation for some plant traits (Fajardo and Siefert, 2016). In arctic tundra, deciduous shrubs,

graminoids and forbs showed approximately two-fold variation in foliar nitrogen values over the growing season (Kelsey et al., 2023). As well, different species may progress through key phenological stages asynchronistically (Bloomfield et al., 2018; Fajardo and Siefert, 2016; McKown et al., 2013). As such, functional composition of the plots, as well as traits of constituent species, evolve over the growing season (Ma et al., 2020; Wang et al., 2022). Using spectral reflectance from a single point in a time in the growing season therefore presents challenges as different species within plots are captured at differing points in their respective phenological path, which may not be the most spectrally discriminative part of the growing season (Beamish et al., 2017).

In addition to individual species phenology, the presence and relative influence of other factors known to contribute to variability in spectral reflectance – factors such as the proportion of non-vascular species, standing litter within the plot and soil moisture concentrations – also evolve over the course of the growing season. For instance, high in situ soil moisture conditions can depress near-infrared (NIR) signals (Jiang et al., 2016), whilst high proportions of standing litter can disproportionately increase NIR reflectance (van Leeuwen and Huete, 1996), introducing further intra-annual variability in spectral reflectance. Between year differences in environmental conditions further compound plant species' and traits' phenological pathways, in turn reducing the inter-annual comparability of spectral data. Indeed, within our study site the 2017/18 and 2018/19 winter snowpacks were respectively very low and high, thus some aspects of drought stress may have been apparent in the leaf spectra in 2017/18, even at peak season, while the 2018/19 development was delayed relative to a more typical year.

Differences in the timing of spectral data acquisition among years exacerbate the challenges in using this technology for long-term monitoring. NEON aims to collect hyperspectral data at each site during peak greenness, however shared equipment, solar angle and cloud cover requirements pose additional constraints such that approximately a quarter of acquisitions to date have occurred outside the actual peak greenness window (Musinsky et al., 2022). At Niwot, acquisitions have typically fallen outside of the optimum timing, with only the 2020 acquisitions beginning within both the (targeted) mean 2003–2021 peak greenness window (measured by MODIS) and the observed period of annual peak greenness (measured by phenocams in tundra on Niwot Ridge) (Fig. 2). 2017 was a particularly poor year for data collection with acquisition not taking place until 47 days after the end of the measured peak greenness window (Fig. 2) (Musinsky et al., 2022). This was evident in all our results where spectral and NDVI dissimilarities were notably low in 2017 (Fig. 3a; 4a,b; 5a,c,e; Supplementary Materials 10). It is likely that a substantial proportion of the annual growth in 2017 had senesced by the time of the NEON flights, which would contribute to the decoupling of spectral signals, particularly the inter-annual signal in NDVI versus field measurements of productivity (Wang et al., 2022). The hyperspectral mosaic product combines individual flights that may have been sampled days or even weeks apart (NEON, 2023a). This could introduce further variability to the hyperspectral comparisons and magnifying the influence of intra-annual compositional and trait plasticity.

Targeting peak phenology periods in mountainous environments is particularly complicated by the strong elevational gradients evident in their phenology, which makes the distinguishing of a single period of peak phenology difficult (Dai et al., 2021; Inouye and Wielgolaski, 2013). When collection dates fall sufficiently late in the season, as those in 2017 did, the spectral data collection may miss the majority of the alpine tundra growing season entirely. As such, key discriminatory signals in the spectra may be lost. Furthermore, whilst the day of peak greenness is relatively stable in tundra ecosystems compared to other ecosystem types (Musinsky et al., 2022), the consequences of flying outside the preferred window to data quality are likely greater. This is because of the steep, rapid changes in both tundra spectra and traits after the peak season with the onset and rapid progression of vegetation senescence (May et al., 2017). Furthermore, even on the selected day of acquisition, factors such as atmospheric conditions, bidirectional reflectance distribution function (BRDF) effects and the timing of the solar noon add further complications to the collection of spectral time series data comparable across years (Jafarbiglu and Pourreza, 2023; Roy et al., 2016).

Characteristics of the in-situ measurement campaigns used here likely also contribute to temporal mismatches. Characterisation of functional composition relies on two primary data sources: composition data and trait data (Ricotta and Pavoine, 2022). Ideally, both plant trait and composition data could be collected at regular intervals across the growing season to facilitate consistent analyses of spectra (Ma et al., 2020). The collection of in situ plant trait data however is extremely time consuming and laborious (Ma et al., 2020) so trait data is rarely collected with such temporal resolution (Jetz et al., 2016). It is typical therefore to rely on taxonomically and spatially gap-filled datasets (Supplementary Materials 2) collected at a limited number of time points. For example, in our study, we relied on data collected at irregular intervals throughout 2008–2009, 2017–2018 and 2021, instead of annually coinciding with the 2017–2020 flight campaigns. The temporal offset in the trait data likely diminishes its quality for use as in situ functional calibration data (Sandel et al., 2015). Thus, it is possible that with more temporally intensive in-situ field campaigns the relationships between spectral and functional β-diversity might be improved. Minimising GPS inaccuracies is also essential to ensure maximum comparability between in situ and remotely sensed data, although negligible differences in spectra extracted using 0 m, 1 m and 3 m buffers (Supplementary Materials 3) suggest that this was not an issue in this study. To say with certainty whether spectral dissimilarity can or cannot be used to monitor changes in functional β-diversity may require more intensive and temporally coherent within-season temporal sampling for both the remote- and both in situ components of the study (Gholizadeh et al., 2019).

4.4. Spectra perform well with biomass

In this study, spectral dissimilarity was more strongly related to biomass dissimilarity than either functional or taxonomic dissimilarity across space. Past studies have successfully established relationships between spectral reflectance and biomass so this result is perhaps unsurprising (Wang et al., 2016b). A plant community's spectral reflectance is defined by the corresponding scattering and absorption of light within, which in turn drives both its chemical and three-dimensional physical structures (Schweiger et al., 2015; Ustin et al., 2004). It therefore follows that the greater the difference in biomass between plots, the greater the likely difference in physical structure and corresponding reflectance. As such, the spectral dissimilarity will be bigger, reflecting the difference in biomass within. Our study supports this application, although only over space where the strength of relationships observed was strong. Relationships between NDVI and biomass dissimilarity were similarly strong within our relatively low biomass study site, however, the strength of such relationships may likely be lower in higher biomass sites where NDVI saturation is more common. Tundra landscapes typically include large proportions of dead plant material, bare ground and disturbance (Nelson et al., 2022; Yang et al., 2020), all factors that may weaken relationships between spectral reflectance, biomass and biodiversity (Rossi et al., 2022; Schweiger et al., 2015).

4.5. What are the alternatives?

Given the moderate strength of the spatial relationships between spectral, functional and taxonomic dissimilarity in this study, and lack of relationships over time, it is worth considering spectral scale and whether the investment in equipment that can capture full-range spectral data is even necessary to monitor change in β-diversity, or whether

simpler, pre-existing technology and metrics would characterise the relationships equally well. In our study, functional, taxonomic and biomass dissimilarity displayed similar relationships with NDVI dissimilarity as they did with spectral dissimilarity in terms of the direction of the relationships and statistical significance. The strength of the relationships between NDVI dissimilarity, and functional and biomass dissimilarity was however notably weaker in all years. This suggests that spectral dissimilarity does capture some functionally relevant information beyond those reflected in NDVI. Past studies have found mixed evidence to this end (Rossi et al., 2022), with some (e.g. Rocchini, 2007) supporting the conclusion that adding spectral bands beyond those present in multispectral imagery enhances the accuracy of spectral biodiversity characterisation, and others not (e.g. Wang et al., 2018). Further studies cataloguing the influence of spectral scale (bandwidth, position and range) to detect different dimensions of biodiversity change (taxonomic vs functional; α vs β-diversity) across a variety of ecosystem types are fundamental to understanding biodiversity-spectral diversity relationships and providing more generalizable guidelines for targeting optical instrumentation for particular biodiversity monitoring applications (Gamon et al., 2020).

Whether the improvements justify the increased cost and complexity of the additional bands likely depends on the intended monitoring application. For characterising beta-diversity across study sites with dramatic variability in above-ground structure – such as across the sub-alpine/tundra ecotone – we would expect to see strong relationships between spectral and taxonomic or functional β-diversity. Indeed, a comparative study across all NEON sites found that spectral-taxonomic dissimilarity relationships were among the strongest at Niwot Ridge of all NEON sites (Schweiger and Laliberté, 2022). Notably, Schweiger and Laliberte's analysis included plots that span multiple ecosystem types (forest, tundra etc.) within a single study area. Whether taxonomic β-diversity across these broad gradients could be detected equally well using NDVI alone, or in conjunction with LiDAR, has not been tested. We calculated NDVI using the same wavelengths as that calculated from Sentinel-2 multispectral imagery (European Space Agency, 2023b), a free, global and temporally dense dataset with 10 m spatial resolution and a return interval of 5 days. Given the wide availability and relative simplicity of multispectral imagery over hyperspectral, perhaps in certain scenarios, using the simpler measure over a larger temporal and geographical expanse is a more worthwhile endeavour, despite the moderate reduction in signal strength.

Even beyond NDVI, other simpler, cheaper methods have proved valuable in the remote characterisation of community diversity. For instance, using specific highly discriminant bands from full-range spectra have proven valuable in characterising tundra diversity (Bratsch et al., 2016; Rossi et al., 2022; Schweiger et al., 2018), whilst airborne LiDAR data, readily available across NEON sites (NEON, 2023b), have been proven to accurately predict tundra shrub biomass (Greaves et al., 2016). Perhaps then the significant expense and complexity of full-range spectrometers are not justified in some instances, and simpler multispectral, LiDAR, or even RGB methods (Beamish et al., 2018) may be similarly effective at delineating aspects of tundra diversity in certain scenarios (Harris et al., 2018). We acknowledge that this is a rapidly developing field and ever-improving processes, methodologies and datasets will only increase the utility of hyperspectral data in biodiversity characterisation in the future. As well, spectral data may prove more useful for other applications than those explored here, such as quantifying canopy nitrogen or water content (Asner and Martin, 2009; Wang et al., 2018). We encourage future studies evaluating the utility of hyperspectral data for monitoring applications to assess not only the performance of hyperspectral data, but also the relative gains over other methods that do not rely on full spectra data.

The question of alternative methods also raises the possibility of boosting performance by the incorporation of additional, non-spectral data sources (Ma et al., 2020). For instance, the fusion of spectral and LiDAR data from remotely sensed platforms has been shown to enhance the characterisation of key vegetation parameters, such as biomass and productivity (Asner et al., 2012; Sankey et al., 2018; Torabzadeh et al., 2014). Fusing spectral data with data on the ecosystem's vertical structure, can dramatically enhance the ecological interpretation of the spectra by facilitating the incorporation of sub-canopy information (Jetz et al., 2016), thereby negating a key limitation of optical data (Ma et al., 2020). LiDAR data is readily available across all NEON sites, although the data from Niwot is insufficient for use in these analyses due to NEON's processing algorithm which rounds all vegetation heights below 2 m to 0 m due to uncertainties in the collected data (Scholl, 2019). Such fusion approaches may be the key to unlocking new satellite-borne hyperspectral platforms – such as the scheduled 'CHIME' (European Space Agency, 2023a). As such, data fusion may enhance the utility of hyperspectral imagery and allow it to fulfil its anticipated promise as the means through which function and biodiversity can be characterised at the biome-scale.

5. Conclusions

In sum, our data support the use of spectral dissimilarity based on hyperspectral campaigns to detect taxonomically and functionally unique areas of the landscape. We do however acknowledge that this application is in part likely to be affected by a degree of noise, highlighted by the moderate relationships between spectral reflectance and in situ dissimilarity metrics over space. Still, we envision that spectral dissimilarity could be readily applied to prioritise spectrally distinct areas for in situ monitoring campaigns. However, the utility of hyperspectral imagery in detecting inter-annual change in alpine tundra composition, functional or taxonomic, remains limited due to methodological limitations, data deficiencies, and inherent mismatches in the acquisition of data across and between growing seasons. The lack of robust relationships identified over time is also a cautionary tale for those attempting to adopt the principles of space-for-time substitution in hyperspectral studies, as with many domains (Blois et al., 2013; Davison et al., 2021). It is important to consider and revisit these identified temporal issues as longer time series emerge to see how much of the anticipated promise of hyperspectral imagery is manifest in long-term monitoring. The lack of robust temporal patterns observed and issues surrounding temporal monitoring using airborne hyperspectral imagery however, do not negate the validity of our study. This work is among the first to use a hyperspectral time series to observe change in vegetation β-diversity over time (Gholizadeh et al., 2020) and paves the way for future studies incorporating longer, more rigorous and more comparable time series.

We attempted to detect and characterise fine-scale changes within a small area of a single tundra vegetation community, an environment known to encompass considerable sub-pixel heterogeneity in composition and function and strong interspecific phenological variation (Bloomfield et al., 2018; Fajardo and Siefert, 2016; McKown et al., 2013; Nelson et al., 2022; Yang et al., 2020). Most plots in our study area were dominated by graminoids and forbs. Thus, the functional dissimilarity was relatively subtle as compared to what might be encountered in other tundra regions, which often also include more lichen, bryophyte, or shrub dominated patches. The limits of hyperspectral remote sensing for change detection encountered here may be similar in other graminoid-dominated systems, which exhibit relatively homogeneous physiognomy and small size of individuals relative to that of pixels. Whilst our ability to characterise such fine-scale change was limited, others have shown spectral and taxonomic β-diversity to strongly relate to one another at larger scales. This includes (Schweiger and Laliberté, 2022) who at the same field location, Niwot Ridge, utilised considerably larger plots (~ 20 × 20 m) across strongly dissimilar ecosystem types (encompassing both tundra and boreal forest) to detect such relationships. Consequently, hyperspectral platforms' most useful avenues may currently lie in large-scale vegetation characterisation and monitoring of

ecosystem change. This includes the characterisation of processes such as treeline expansion and warming-induced shrubification (Grigoriev et al., 2022; Jia et al., 2022) but also more widely vegetation classification and the direct observation of tundra functional traits (Thomson et al., 2021). It could be argued that platforms including LiDAR and simpler optical measures (e.g. NDVI) perform these functions equally well already (Berner et al., 2020; Myers-Smith et al., 2020) and that the added utility of hyperspectral imaging does not yet justify its utility. This study suggests that hyperspectral imagery does provide notable additional benefits in the characterisation of fine-scale tundra functional β-diversity across space, but that advances are required in methodology and data acquisition if we are to extract the full potential of hyperspectral time series in biodiversity science.

CRediT authorship contribution statement

Joseph J. Everest: Writing – original draft, Visualization, Validation, Resources, Project administration, Methodology, Investigation, Formal analysis, Data curation, Conceptualization. **Elisa Van Cleemput:** Writing – review & editing, Methodology, Investigation, Formal analysis. **Alison L. Beamish:** Writing – review & editing, Methodology. **Marko J. Spasojevic:** Writing – review & editing, Data curation. **Hope C. Humphries:** Formal analysis. **Sarah C. Elmendorf:** Writing – review & editing, Visualization, Supervision, Methodology, Investigation, Funding acquisition, Formal analysis, Data curation, Conceptualization.

Declaration of competing interest

The authors declare that they have no known competing financial interests or personal relationships that could have appeared to influence the work reported in this paper.

Data availability

Data and code has been made available at the following GitHub repository: https://github.com/josephjeverest/hyperspec_turnover.

Acknowledgements

This project was kindly supported by the UK Natural Environment Research Council's and University of Edinburgh's E4 Doctoral Training Programme Research Training Support Grant and Overseas Research Visit and Conference fund. This project was also supported by the Niwot Ridge LTER program (NSF DEB-1637686; NSF DEB-2224439). The National Ecological Observatory Network is a program sponsored by the National Science Foundation and operated under cooperative agreement by Battelle. This material is based in part upon work supported by the National Science Foundation through the NEON Program. We are particularly grateful to Bridget Hass and Claire Lunch for the code and expertise they provided when working with the spectroscopy data. We are also grateful to our data contributors, including NEON, the Niwot Ridge LTER and all the individuals who collected data in the field.

Appendix A. Supplementary data

Supplementary data to this article can be found online at https://doi.org/10.1016/j.rse.2024.114507.

References

Anderson, C.B., 2018. Biodiversity monitoring, earth observations and the ecology of scale. Ecol. Lett. 21, 1572–1585. https://doi.org/10.1111/ele.13106.

Anderson, M.J., Crist, T.O., Chase, J.M., Vellend, M., Inouye, B.D., Freestone, A.L., Sanders, N.J., Cornell, H.V., Comita, L.S., Davies, K.F., Harrison, S.P., Kraft, N.J.B., Stegen, J.C., Swenson, N.G., 2011. Navigating the multiple meanings of β diversity: a roadmap for the practicing ecologist. Ecol. Lett. 14, 19–28. https://doi.org/10.1111/j.1461-0248.2010.01552.x.

Asner, G.P., Martin, R.E., 2009. Airborne spectranomics: mapping canopy chemical and taxonomic diversity in tropical forests. Front. Ecol. Environ. 7, 269–276. https://doi.org/10.1890/070152.

Asner, G.P., Knapp, D.E., Boardman, J., Green, R.O., Kennedy-Bowdoin, T., Eastwood, M., Martin, R.E., Anderson, C., Field, C.B., 2012. Carnegie airborne Observatory-2: increasing science data dimensionality via high-fidelity multi-sensor fusion. Remote Sens. Environ. 124, 454–465. https://doi.org/10.1016/j.rse.2012.06.012.

Asner, G.P., Martin, R.E., Knapp, D.E., Tupayachi, R., Anderson, C.B., Sinca, F., Vaughn, N.R., Llactayo, W., 2017. Airborne laser-guided imaging spectroscopy to map forest trait diversity and guide conservation. Science 355, 385–389. https://doi.org/10.1126/science.aaj1987.

Baldeck, C.A., Asner, G.P., 2013. Estimating vegetation beta diversity from airborne imaging spectroscopy and unsupervised clustering. Remote Sens. (Basel) 5, 2057–2071. https://doi.org/10.3390/rs5052057.

Beamish, A.L., Coops, N., Chabrillat, S., Heim, B., 2017. A phenological approach to spectral differentiation of low-arctic tundra vegetation communities, north slope, Alaska. Remote Sens. 9, 1200. https://doi.org/10.3390/rs9111200.

Beamish, A.L., Coops, N.C., Hermosilla, T., Chabrillat, S., Heim, B., 2018. Monitoring pigment-driven vegetation changes in a low-Arctic tundra ecosystem using digital cameras. Ecosphere 9, e02123. https://doi.org/10.1002/ecs2.2123.

Beccari, E., Pérez Carmona, C., Tordoni, E., Petruzzellis, F., Martinucci, D., Casagrande, G., Pavanetto, N., Rocchini, D., D'Antraccoli, M., Ciccarelli, D., Bacaro, G., 2024. Plant spectral diversity from high-resolution multispectral imagery detects functional diversity patterns in coastal dune communities. J. Veg. Sci. 35 (2), e13239.

Berner, L.T., Massey, R., Jantz, P., Forbes, B.C., Macias-Fauria, M., Myers-Smith, I., Kumpula, T., Gauthier, G., Andreu-Hayles, L., Gaglioti, B.V., Burns, P., Zetterberg, P., D'Arrigo, R., Goetz, S.J., 2020. Summer warming explains widespread but not uniform greening in the Arctic tundra biome. Nat. Commun. 11, 4621. https://doi.org/10.1038/s41467-020-18479-5.

Bishop, T.R., Robertson, M.P., van Rensburg, B.J., Parr, C.L., 2015. Contrasting species and functional beta diversity in montane ant assemblages. J. Biogeogr. 42, 1776–1786. https://doi.org/10.1111/jbi.12537.

Bjorkman, A.D., Myers-Smith, I.H., Elmendorf, S.C., Normand, S., Rüger, N., Beck, P.S.A., Blach-Overgaard, A., Blok, D., Cornelissen, J.H.C., Forbes, B.C., Georges, D., Goetz, S.J., Guay, K.C., Henry, G.H.R., HilleRisLambers, J., Hollister, R.D., Karger, D.N., Kattge, J., Manning, P., Prevéy, J.S., Rixen, C., Schaepman-Strub, G., Thomas, H.J. D., Vellend, M., Wilmking, M., Wipf, S., Carbognani, M., Hermanutz, L., Lévesque, E., Molau, U., Petraglia, A., Soudzilovskaia, N.A., Spasojevic, M.J., Tomaselli, M., Vowles, T., Alatalo, J.M., Alexander, H.D., Anadon-Rosell, A., Angers-Blondin, S., Beest, M. te, Berner, L., Björk, R.G., Buchwal, A., Buras, A., Christie, K., Cooper, E.J., Dullinger, S., Elberling, B., Eskelinen, A., Frei, E.R., Grau, O., Grogan, P., Hallinger, M., Harper, K.A., Heijmans, M.M.P.D., Hudson, J., Hülber, K., Iturrate-Garcia, M., Iversen, C.M., Jaroszynska, F., Johnstone, J.F., Jørgensen, R.H., Kaarlejärvi, E., Klady, R., Kuleza, S., Kulonen, A., Lamarque, L.J., Lantz, T., Little, C.J., Speed, J.D. M., Michelsen, A., Milbau, A., Nabe-Nielsen, J., Nielsen, S.S., Ninot, J.M., Oberbauer, S.F., Olofsson, J., Onipchenko, V.G., Rumpf, S.B., Semenchuk, P., Shetti, R., Collier, L.S., Street, L.E., Suding, K.N., Tape, K.D., Trant, A., Treier, U.A., Tremblay, J.-P., Tremblay, M., Venn, S., Weijers, S., Zamin, T., Boulanger-Lapointe, N., Gould, W.A., Hik, D.S., Hofgaard, A., Jónsdóttir, I.S., Jorgenson, J., Klein, J., Magnusson, B., Tweedie, C., Wookey, P.A., Bahn, M., Blonder, B., van Bodegom, P.M., Bond-Lamberty, B., Campetella, G., Cerabolini, B.E.L., Chapin, F.S., Cornwell, W.K., Craine, J., Dainese, M., de Vries, F.T., Díaz, S., Enquist, B.J., Green, W., Milla, R., Niinemets, Ü., Onoda, Y., Ordoñez, J.C., Ozinga, W.A., Penuelas, J., Poorter, H., Poschlod, P., Reich, P.B., Sandel, B., Schamp, B., Sheremetev, S., Weiher, E., 2018. Plant functional trait change across a warming tundra biome. Nature 562, 57–62. doi:https://doi.org/10.1038/s41586-018-0563-7.

Blois, J.L., Williams, J.W., Fitzpatrick, M.C., Jackson, S.T., Ferrier, S., 2013. Space can substitute for time in predicting climate-change effects on biodiversity. Proc. Natl. Acad. Sci. 110, 9374–9379. https://doi.org/10.1073/pnas.1220228110.

Bloomfield, K.J., Cernusak, L.A., Eamus, D., Ellsworth, D.S., Colin Prentice, I., Wright, I. J., Boer, M.M., Bradford, M.G., Cale, P., Cleverly, J., 2018. A continental-scale assessment of variability in leaf traits: within species, across sites and between seasons. Funct. Ecol. 32, 1492–1506.

Blowes, S.A., Supp, S.R., Antão, L.H., Bates, A., Bruelheide, H., Chase, J.M., Moyes, F., Magurran, A., McGill, B., Myers-Smith, I.H., Winter, M., Bjorkman, A.D., Bowler, D. E., Byrnes, J.E.K., Gonzalez, A., Hines, J., Isbell, F., Jones, H.P., Navarro, L.M., Thompson, P.L., Vellend, M., Waldock, C., Dornelas, M., 2019. The geography of biodiversity change in marine and terrestrial assemblages. Science 366, 339–345. https://doi.org/10.1126/science.aaw1620.

Bratsch, S.N., Epstein, H.E., Buchhorn, M., Walker, D.A., 2016. Differentiating among four arctic tundra plant communities at Ivotuk, Alaska using field spectroscopy. Remote Sens. 8, 51. https://doi.org/10.3390/rs8010051.

Bray, J.R., Curtis, J.T., 1957. An ordination of the upland forest communities of southern Wisconsin. Ecological monographs 27, 325–349. https://doi.org/10.2307/1942268.

Carlson, K.M., Asner, G.P., Hughes, R.F., Ostertag, R., Martin, R.E., 2007. Hyperspectral remote sensing of canopy biodiversity in Hawaiian lowland rainforests. Ecosystems 10, 536–549. https://doi.org/10.1007/s10021-007-9041-z.

Chauhan, H., Krishna Mohan, B., 2014. Effectiveness of spectral similarity measures to develop precise crop spectra for hyperspectral data analysis. ISPRS Ann. Photogramm. Remote Sens. Spat Inform. Sci. II–8, 83–90. https://doi.org/10.5194/isprsannals-II-8-83-2014.

Dahlin, K.M., Asner, G.P., Field, C.B., 2013. Environmental and community controls on plant canopy chemistry in a Mediterranean-type ecosystem. Proc. Natl. Acad. Sci. 110, 6895–6900. https://doi.org/10.1073/pnas.1215513110.

Dai, J., Zhu, M., Mao, W., Liu, R., Wang, H., Alatalo, J.M., Tao, Z., Ge, Q., 2021. Divergent changes of the elevational synchronicity in vegetation spring phenology in North China from 2001 to 2017 in connection with variations in chilling. Int. J. Climatol. 41, 6109–6121. https://doi.org/10.1002/joc.7170.

Davison, C.W., Rahbek, C., Morueta-Holme, N., 2021. Land-use change and biodiversity: challenges for assembling evidence on the greatest threat to nature. Glob. Change Biol. 27, 5414–5429. https://doi.org/10.1111/gcb.15846.

Díaz, S., Cabido, M., 2001. Vive la différence: plant functional diversity matters to ecosystem processes. Trends Ecol. Evol. 16, 646–655. https://doi.org/10.1016/S0169-5347(01)02283-2.

European Space Agency, 2023a. Going Hyperspectral for CHIME [WWW Document]. https://www.esa.int/Applications/Observing_the_Earth/Copernicus/Going_hyperspectral_for_CHIME (accessed 4.7.23).

European Space Agency, 2023b. Sentinel-2 - Missions - Resolution and Swath - Sentinel Handbook [WWW Document]. Sentin. Online. https://copernicus.eu/missions/sentinel-2/instrument-payload/resolution-and-swath (accessed 4.7.23).

Fajardo, A., Siefert, A., 2016. Phenological variation of leaf functional traits within species. Oecologia 180, 951–959.

Feilhauer, H., Asner, G.P., Martin, R.E., Schmidtlein, S., 2010. Brightness-normalized partial least squares regression for hyperspectral data. J. Quant. Spectrosc. Radiat. Transf. 111, 1947–1957. https://doi.org/10.1016/j.jqsrt.2010.03.007.

Féret, J.-B., Asner, G.P., 2014. Mapping tropical forest canopy diversity using high-fidelity imaging spectroscopy. Ecol. Appl. Publ. Ecol. Soc. Am. 24, 1289–1296. https://doi.org/10.1890/13-1824.1.

Féret, J.-B., De Boissieu, F., 2020. biodivMapR: an r package for α-and β-diversity mapping using remotely sensed images. Methods Ecol. Evol. 11, 64–70.

Gallery, W., 2022. Neon Algorithm Theoretical Basis Document (ATBD): Spectrometer Mosaic [WWW Document]. https://data.neonscience.org/data-products/DP3.30006.001/RELEASE-2024 (accessed 10.27.24).

Gamon, J.A., Somers, B., Malenovský, Z., Middleton, E.M., Rascher, U., Schaepman, M.E., 2019. Assessing vegetation function with imaging spectroscopy. Surv. Geophys. 40, 489–513. https://doi.org/10.1007/s10712-019-09511-5.

Gamon, J.A., Wang, R., Gholizadeh, H., Zutta, B., Townsend, P.A., Cavender-Bares, J., 2020. Consideration of scale in remote sensing of biodiversity. Remote Sens. Plant Biodivers. 425–447.

Gamon, J.A., Wang, R., Russo, S.E., 2023. Contrasting photoprotective responses of forest trees revealed using PRI light responses sampled with airborne imaging spectrometry. New Phytol. 238, 1318–1332. https://doi.org/10.1111/nph.18754.

Gholizadeh, H., Gamon, J.A., Townsend, P.A., Zygielbaum, A.I., Helzer, C.J., Hmimina, G.Y., Yu, R., Moore, R.M., Schweiger, A.K., Cavender-Bares, J., 2019. Detecting prairie biodiversity with airborne remote sensing. Remote Sens. Environ. 221, 38–49. https://doi.org/10.1016/j.rse.2018.10.037.

Gholizadeh, H., Gamon, J.A., Helzer, C.J., Cavender-Bares, J., 2020. Multi-temporal assessment of grassland α- and β-diversity using hyperspectral imaging. Ecol. Appl. 30, e02145. https://doi.org/10.1002/eap.2145.

Gillespie, T.W., Foody, G.M., Rocchini, D., Giorgi, A.P., Saatchi, S., 2008. Measuring and modelling biodiversity from space. Prog. Phys. Geogr. 32, 203–221.

Goswami, S., Gamon, J., Vargas, S., Tweedie, C., 2015. *Relationships of NDVI, Biomass, and Leaf Area Index (LAI) for six key plant species in Barrow, Alaska* (No. e913v1). PeerJ PrePrints.

Greaves, H.E., Vierling, L.A., Eitel, J.U.H., Boelman, N.T., Magney, T.S., Prager, C.M., Griffin, K.L., 2016. High-resolution mapping of aboveground shrub biomass in Arctic tundra using airborne lidar and imagery. Remote Sens. Environ. 184, 361–373. https://doi.org/10.1016/j.rse.2016.07.026.

Grigoriev, A.A., Shalaumova, Y.V., Balakin, D.S., Erokhina, O.V., Abdulmanova, S.Y., Moiseev, P.A., Camarero, J.J., 2022. Alpine shrubification: juniper encroachment into tundra in the Ural mountains. Forests 13, 2106. https://doi.org/10.3390/f13122106.

Haboudane, D., Miller, J.R., Pattey, E., Zarco-Tejada, P.J., Strachan, I.B., 2004. Hyperspectral vegetation indices and novel algorithms for predicting green LAI of crop canopies: modeling and validation in the context of precision agriculture. Remote Sens. Environ. 90, 337–352. https://doi.org/10.1016/j.rse.2003.12.013.

Häger, A., Avalos, G., 2017. Do functional diversity and trait dominance determine carbon storage in an altered tropical landscape? Oecologia 184, 569–581. https://doi.org/10.1007/s00442-017-3880-x.

Harris, D.J., Taylor, S.D., White, E.P., 2018. Forecasting biodiversity in breeding birds using best practices. PeerJ 6, e4278. https://doi.org/10.7717/peerj.4278.

He, K., Zhang, J., 2009. Testing the correlation between beta diversity and differences in productivity among global ecoregions, biomes, and biogeographical realms. Ecol. Inform. 4, 93–98. https://doi.org/10.1016/j.ecoinf.2009.01.003.

He, K.S., Zhang, J., Zhang, Q., 2009. Linking variability in species composition and MODIS NDVI based on beta diversity measurements. Acta Oecol. 35, 14–21. https://doi.org/10.1016/j.actao.2008.07.006.

Homolová, L., Malenovský, Z., Clevers, J.G.P.W., García-Santos, G., Schaepman, M.E., 2013. Review of optical-based remote sensing for plant trait mapping. Ecol. Complex. 15, 1–16. https://doi.org/10.1016/j.ecocom.2013.06.003.

Imbert, J.B., Blanco, J.A., Candel-Pérez, D., Lo, Y.-H., González de Andrés, E., Yeste, A., Herrera-Álvarez, X., Rivadeneira Barba, G., Liu, Y., Chang, S.-C., 2021. Synergies between climatechange, biodiversity, ecosystem function and services, indirect drivers of change and human well-being in forests. In: Venkatramanan, V., Shah, S., Prasad, R. (Eds.), Exploring Synergies and Trade-Offs between Climate Change and the Sustainable Development Goals. Springer, Singapore, pp. 263–320. https://doi.org/10.1007/978-981-15-7301-9_12.

Inamdar, D., Kalacska, M., Leblanc, G., Arroyo-Mora, J.P., 2020. Characterizing and mitigating sensor generated spatial correlations in airborne hyperspectral imaging data. Remote Sens. (Basel) 12, 641. https://doi.org/10.3390/rs12040641.

Inouye, D.W., Wielgolaski, F.E., 2013. Phenology at high altitudes. In: Schwartz, M.D. (Ed.), Phenology: An Integrative Environmental Science. Springer, Netherlands, Dordrecht, pp. 249–272. https://doi.org/10.1007/978-94-007-6925-0_14.

Jafarbiglu, H., Pourreza, A., 2023. Impact of sun-view geometry on canopy spectral reflectance variability. ISPRS J. Photogramm. Remote Sens. 196, 270–286. https://doi.org/10.1016/j.isprsjprs.2022.12.002.

Jetz, W., Cavender-Bares, J., Pavlick, R., Schimel, D., Davis, F.W., Asner, G.P., Guralnick, R., Kattge, J., Latimer, A.M., Moorcroft, P., Schaepman, M.E., Schildhauer, M.P., Schneider, F.D., Schrodt, F., Stahl, U., Ustin, S.L., 2016. Monitoring plant functional diversity from space. Nat. Plants 2, 1–5. https://doi.org/10.1038/nplants.2016.24.

Jia, B., Jia, L., Mou, X.M., Chen, J., Li, F.-C., Ma, Q., Li, X.G., 2022. Shrubification decreases soil organic carbon mineralization and its temperature sensitivity in alpine meadow soils. Soil Biol. Biochem. 168, 108651. https://doi.org/10.1016/j.soilbio.2022.108651.

Jiang, Q., Chen, Y., Guo, L., Fei, T., Qi, K., 2016. Estimating soil organic carbon of cropland soil at different levels of soil moisture using VIS-NIR spectroscopy. Remote Sens. (Basel) 8, 755. https://doi.org/10.3390/rs8090755.

Karpowicz, B., Kampe, T., 2022. Neon Imaging Spectrometer Radiance To Reflectance Algorithm Theoretical Document [Www Document]. https://data.neonscience.org/data-products/DP3.30006.001/RELEASE-2024.

Kelsey, K.C., Højlund Pedersen, S., Leffler, A.J., Sexton, J.O., Welker, J.M., 2023. Snow and vegetation seasonality influence seasonal trends of leaf nitrogen and biomass in Arctic tundra. Ecosphere 14, e4515. https://doi.org/10.1002/ecs2.4515.

Kishore, B.S.P.C., Kumar, A., Saikia, P., Khan, M.L., 2023. Alpha and beta diversity mapping in Indian tropical deciduous forests using high-fidelity imaging spectroscopy. Adv. Space Res. https://doi.org/10.1016/j.asr.2023.02.031.

Laliberté, E., Schweiger, A.K., Legendre, P., 2020. Partitioning plant spectral diversity into alpha and beta components. Ecol. Lett. 23, 370–380. https://doi.org/10.1111/ele.13429.

Lavorel, S., Díaz, S., Cornelissen, J.H.C., Garnier, E., Harrison, S.P., McIntyre, S., Pausas, J.G., Pérez-Harguindeguy, N., Roumet, C., Urcelay, C., 2007. Plant functional types: Are we getting any closer to the holy grail? In: Canadell, J.G., Pataki, D.E., Pitelka, L.F. (Eds.), Terrestrial Ecosystems in a Changing World, Global Change — The IGBP Series. Springer, Berlin, Heidelberg, pp. 149–164. https://doi.org/10.1007/978-3-540-32730-1_13.

van Leeuwen, W.J.D., Huete, A.R., 1996. Effects of standing litter on the biophysical interpretation of plant canopies with spectral indices. Remote Sens. Environ. 55, 123–138. https://doi.org/10.1016/0034-4257(95)00198-0.

Lopatin, J., Fassnacht, F.E., Kattenborn, T., Schmidtlein, S., 2017. Mapping plant species in mixed grassland communities using close range imaging spectroscopy. Remote Sens. Environ. 201, 12–23.

Ma, X., Migliavacca, M., Wirth, C., Bohn, F.J., Huth, A., Richter, R., Mahecha, M.D., 2020. Monitoring plant functional diversity using the reflectance and echo from space. Remote Sens. (Basel) 12, 1248. https://doi.org/10.3390/rs12081248.

Maitner, B.S., Halbritter, A.H., Telford, R.J., Strydom, T., Chacon, J., Lamanna, C., Sloat, L.L., Kerkhoff, A.J., Messier, J., Rasmussen, N., Pomati, F., Merz, E., Vandvik, V., Enquist, B.J., 2023. Bootstrapping outperforms community-weighted approaches for estimating the shapes of phenotypic distributions. Methods Ecol. Evol. 14, 2592–2610. https://doi.org/10.1111/2041-210X.14160.

Mantel, N., 1967. The detection of disease clustering and a generalized regression approach. Cancer Res. 27, 209–220.

Marzialetti, F., Cascone, S., Frate, L., Di Febbraro, M., Acosta, A.T.R., Carranza, M.L., 2021. Measuring alpha and beta diversity by field and remote-sensing data: a challenge for coastal dunes biodiversity monitoring. Remote Sens. (Basel) 13, 1928. https://doi.org/10.3390/rs13101928.

May, J.L., Healey, N.C., Ahrends, H.E., Hollister, R.D., Tweedie, C.E., Welker, J.M., Gould, W.A., Oberbauer, S.F., 2017. Short-term impacts of the air temperature on greening and senescence in Alaskan arctic plant tundra habitats. Remote Sens. (Basel) 9, 1338. https://doi.org/10.3390/rs9121338.

McKown, A.D., Guy, R.D., Azam, M.S., Drewes, E.C., Quamme, L.K., 2013. Seasonality and phenology alter functional leaf traits. Oecologia 172, 653–665.

Meng, R., Yang, D., McMahon, A., Hantson, W., Hayes, D., Breen, A., Serbin, S., 2019. A UAS platform for assessing spectral, structural, and thermal patterns of arctic tundra vegetation. In: IGARSS 2019–2019 IEEE International Geoscience and Remote Sensing Symposium. Presented at the IGARSS 2019–2019 IEEE International Geoscience and Remote Sensing Symposium, pp. 9113–9116. https://doi.org/10.1109/IGARSS.2019.8897953.

Miedema Brown, L., Anand, M., 2022. Plant functional traits as measures of ecosystem service provision. Ecosphere 13, e3930. https://doi.org/10.1002/ecs2.3930.

Miller, C.E., Griffith, P.C., Goetz, S.J., Hoy, E.E., Pinto, N., McCubbin, I.B., Thorpe, A.K., Hofton, M., Hodkinson, D., Hansen, C., Woods, J., Larson, E., Kasischke, E.S., Margolis, H.A., 2019. An overview of ABoVE airborne campaign data acquisitions and science opportunities. Environ. Res. Lett. 14, 080201. https://doi.org/10.1088/1748-9326/ab0d44.

Musinsky, J., Goulden, T., Wirth, G., Leisso, N., Krause, K., Haynes, M., Chapman, C., 2022. Spanning scales: the airborne spatial and temporal sampling design of the national ecological observatory network. Methods Ecol. Evol. 13, 1866–1884. https://doi.org/10.1111/2041-210X.13942.

Myers-Smith, I.H., Kerby, J.T., Phoenix, G.K., Bjerke, J.W., Epstein, H.E., Assmann, J.J., John, C., Andreu-Hayles, L., Angers-Blondin, S., Beck, P.S.A., Berner, L.T., Bhatt, U.S., Bjorkman, A.D., Blok, D., Bryn, A., Christiansen, C.T., Cornelissen, J.H.C., Cunliffe, A.M., Elmendorf, S.C., Forbes, B.C., Goetz, S.J., Hollister, R.D., de Jong, R., Loranty, M.M., Macias-Fauria, M., Maseyk, K., Normand, S., Olofsson, J., Parker, T.C., Parmentier, F.-J.W., Post, E., Schaepman-Strub, G., Stordal, F., Sullivan, P.F., Thomas, H.J.D., Tømmervik, H., Treharne, R., Tweedie, C.E., Walker, D.A.,

Wilmking, M., Wipf, S., 2020. Complexity revealed in the greening of the Arctic. Nat. Clim. Chang. 10, 106–117. https://doi.org/10.1038/s41558-019-0688-1.
Nelson, P.R., Maguire, A.J., Pierrat, Z., Orcutt, E.L., Yang, D., Serbin, S., Frost, G.V., Macander, M.J., Magney, T.S., Thompson, D.R., Wang, J.A., Oberbauer, S.F., Zesati, S.V., Davidson, S.J., Epstein, H.E., Unger, S., Campbell, P.K.E., Carmon, N., Velez-Reyes, M., Huemmrich, K.F., 2022. Remote sensing of tundra ecosystems using high spectral resolution reflectance: opportunities and challenges. J. Geophys. Res. Biogeosci. 127, e2021JG006697. https://doi.org/10.1029/2021JG006697.
NEON, 2023a. Spectrometer Orthorectified Surface Directional Reflectance - Mosaic (DP3.30006.001). https://doi.org/10.48443/WZWJ-NM11.
NEON, 2023b. Elevation - LiDAR. https://doi.org/10.48443/KVB6-4322.
NEON, 2023c. High-resolution Orthorectified Camera Imagery Mosaic (DP3.30010.001). https://doi.org/10.48443/67BY-MQ58.
Niwot Ridge, L.T.E.R., 2023. Niwot Ridge LTER [WWW Document]. Niwot Ridge LTER. https://nwt.lternet.edu (accessed 6.17.23).
Osnas, J.L., Katabuchi, M., Kitajima, K., Wright, S.J., Reich, P.B., Van Bael, S.A., Kraft, N. J., Samaniego, M.J., Pacala, S.W., Lichstein, J.W., 2018. Divergent drivers of leaf trait variation within species, among species, and among functional groups. Proceedings of the National Academy of Sciences 115 (21), 5480–5485.
Ottoy, S., Van Meerbeek, K., Sindayihebura, A., Hermy, M., Van Orshoven, J., 2017. Assessing top-and subsoil organic carbon stocks of low-input high-diversity systems using soil and vegetation characteristics. Sci. Total Environ. 589, 153–164.
Park, Y., Noda, I., Jung, Y.M., 2018. Smooth factor analysis (SFA) to effectively remove high levels of noise from spectral data sets. Appl. Spectrosc. 72, 765–775. https://doi.org/10.1177/0003702817752126.
Perez-Harguindeguy, N., Diaz, S., Garnier, E., Lavorel, S., Poorter, H., Jaureguiberry, P., Bret-Harte, M.S., Cornwell, W.K., Craine, J.M., Gurvich, D.E., 2016. Corrigendum to: new handbook for standardised measurement of plant functional traits worldwide. Aust. J. Bot. 64, 715–716.
Ricotta, C., Pavoine, S., 2022. A new parametric measure of functional dissimilarity: bridging the gap between the Bray-Curtis dissimilarity and the Euclidean distance. Ecol. Model. 466, 109880. https://doi.org/10.1016/j.ecolmodel.2022.109880.
Rocchini, D., 2007. Effects of spatial and spectral resolution in estimating ecosystem α-diversity by satellite imagery. Remote sensing of Environment 111 (4), 423–434.
Rocchini, D., He, K.S., Oldeland, J., Wesuls, D., Neteler, M., 2010. Spectral variation versus species β-diversity at different spatial scales: a test in African highland savannas. J. Environ. Monit. 12, 825–831. https://doi.org/10.1039/B921835A.
Rocchini, D., Luque, S., Pettorelli, N., Bastin, L., Doktor, D., Faedi, N., Feilhauer, H., Féret, J.-B., Foody, G.M., Gavish, Y., Godinho, S., Kunin, W.E., Lausch, A., Leitão, P. J., Marcantonio, M., Neteler, M., Ricotta, C., Schmidtlein, S., Vihervaara, P., Wegmann, M., Nagendra, H., 2018. Measuring β-diversity by remote sensing: a challenge for biodiversity monitoring. Methods Ecol. Evol. 9, 1787–1798. https://doi.org/10.1111/2041-210X.12941.
Rossi, C., Kneubühler, M., Schütz, M., Schaepman, M.E., Haller, R.M., Risch, A.C., 2022. Spatial resolution, spectral metrics and biomass are key aspects in estimating plant species richness from spectral diversity in species-rich grasslands. Remote Sens. Ecol. Conserv. 8, 297–314. https://doi.org/10.1002/rse2.244.
Roy, D.P., Zhang, H.K., Ju, J., Gomez-Dans, J.L., Lewis, P.E., Schaaf, C.B., Sun, Q., Li, J., Huang, H., Kovalskyy, V., 2016. A general method to normalize Landsat reflectance data to nadir BRDF adjusted reflectance. Remote Sens. Environ. 176, 255–271. https://doi.org/10.1016/j.rse.2016.01.023.
Rüfenacht, D., Fredembach, C., Süsstrunk, S., 2014. Automatic and accurate shadow detection using near-infrared information. IEEE Trans. Pattern Anal. Mach. Intell. 36, 1672–1678. https://doi.org/10.1109/TPAMI.2013.229.
Sandel, B., Gutiérrez, A.G., Reich, P.B., Schrodt, F., Dickie, J., Kattge, J., 2015. Estimating the missing species bias in plant trait measurements. J. Veg. Sci. 26, 828–838.
Sankey, T.T., McVay, J., Swetnam, T.L., McClaran, M.P., Heilman, P., Nichols, M., 2018. UAV hyperspectral and lidar data and their fusion for arid and semi-arid land vegetation monitoring. Remote Sens. Ecol. Conserv. 4, 20–33. https://doi.org/10.1002/rse2.44.
Schneider, F.D., Morsdorf, F., Schmid, B., Petchey, O.L., Hueni, A., Schimel, D.S., Schaepman, M.E., 2017. Mapping functional diversity from remotely sensed morphological and physiological forest traits. Nat. Commun. 8, 1441. https://doi.org/10.1038/s41467-017-01530-3.
Scholl, V.M., 2019. Assessing the Integration and Pre-Processing of NEON Airborne Remote Sensing and In-Situ Data for Optimal Tree Species Classification. University of Colorado at Boulder.
Schweiger, A.K., Laliberté, E., 2022. Plant beta-diversity across biomes captured by imaging spectroscopy. Nat. Commun. 13, 2767. https://doi.org/10.1038/s41467-022-30369-6.
Schweiger, A.K., Risch, A.C., Damm, A., Kneubühler, M., Haller, R., Schaepman, M.E., Schütz, M., 2015. Using imaging spectroscopy to predict above-ground plant biomass in alpine grasslands grazed by large ungulates. J. Veg. Sci. 26, 175–190. https://doi.org/10.1111/jvs.12214.
Schweiger, A.K., Cavender-Bares, J., Townsend, P.A., Hobbie, S.E., Madritch, M.D., Wang, R., Tilman, D., Gamon, J.A., 2018. Plant spectral diversity integrates functional and phylogenetic components of biodiversity and predicts ecosystem function. Nat. Ecol. Evol. 2, 976–982. https://doi.org/10.1038/s41559-018-0551-1.
Serbin, S.P., Townsend, P.A., 2020. Scaling functional traits from leaves to canopies. Remote Sens. Plant Biodivers. 43–82.
Spasojevic, M.J., Weber, S.E., 2008. Niwot Ridge LTER, 2022. Niwot Plant Functional Traits. https://doi.org/10.6073/PASTA/1A06BCFFA07E7AA2A4B674AF4C427860.
Spasojevic, M.J., Bowman, W.D., Humphries, H.C., Seastedt, T.R., Suding, K.N., 2013. Changes in alpine vegetation over 21 years: are patterns across a heterogeneous landscape consistent with predictions? Ecosphere 4, art117. https://doi.org/10.1890/ES13-00133.1.
Stasinski, L., White, D.M., Nelson, P.R., Ree, R.H., Meireles, J.E., 2021. Reading light: leaf spectra capture fine-scale diversity of closely related, hybridizing arctic shrubs. New Phytol. 232, 2283–2294. https://doi.org/10.1111/nph.17731.
Suding, K.N., Lavorel, S., Chapin Iii, F.S., Cornelissen, J.H.C., Díaz, S., Garnier, E., Goldberg, D., Hooper, D.U., Jackson, S.T., Navas, M.-L., 2008. Scaling environmental change through the community-level: a trait-based response-and-effect framework for plants. Glob. Change Biol. 14, 1125–1140. https://doi.org/10.1111/j.1365-2486.2008.01557.x.
Tagliabue, G., Panigada, C., Dechant, B., Baret, F., Cogliati, S., Colombo, R., Migliavacca, M., Rademske, P., Schickling, A., Schüttemeyer, D., 2019. Exploring the spatial relationship between airborne-derived red and far-red sun-induced fluorescence and process-based GPP estimates in a forest ecosystem. Remote Sens. Environ. 231, 111272.
The Plant List, 2013. Version 1.1. Published on the Internet [WWW Document]. http://www.theplantlist.org/ (accessed 6.4.23).
Thomas, H.J.D., Bjorkman, A.D., Myers-Smith, I.H., Elmendorf, S.C., Kattge, J., Diaz, S., Vellend, M., Blok, D., Cornelissen, J.H.C., Forbes, B.C., Henry, G.H.R., Hollister, R. D., Normand, S., Prevéy, J.S., Rixen, C., Schaepman-Strub, G., Wilmking, M., Wipf, S., Cornwell, W.K., Beck, P.S.A., Georges, D., Goetz, S.J., Guay, K.C., Rüger, N., Soudzilovskaia, N.A., Spasojevic, M.J., Alatalo, J.M., Alexander, H.D., Anadon-Rosell, A., Angers-Blondin, S., te Beest, M., Berner, L.T., Björk, R.G., Buchwal, A., Buras, A., Carbognani, M., Christie, K.S., Collier, L.S., Cooper, E.J., Elberling, B., Eskelinen, A., Frei, E.R., Grau, O., Grogan, P., Hallinger, M., Heijmans, M.M.P.D., Hermanutz, L., Hudson, J.M.G., Johnstone, J.F., Hülber, K., Iturrate-Garcia, M., Iversen, C.M., Jaroszynska, F., Kaarlejarvi, E., Kulonen, A., Lamarque, L.J., Lantz, T. C., Lévesque, E., Little, C.J., Michelsen, A., Milbau, A., Nabe-Nielsen, J., Nielsen, S. S., Ninot, J.M., Oberbauer, S.F., Olofsson, J., Onipchenko, V.G., Petraglia, A., Rumpf, S.B., Shetti, R., Speed, J.D.M., Suding, K.N., Tape, K.D., Tomaselli, M., Trant, A.J., Treier, U.A., Tremblay, M., Venn, S.E., Vowles, T., Weijers, S., Wookey, P.A., Zamin, T.J., Bahn, M., Blonder, B., van Bodegom, P.M., Bond-Lamberty, B., Campetella, G., Cerabolini, B.E.L., Chapin, F.S., Craine, J.M., Dainese, M., Green, W.A., Jansen, S., Kleyer, M., Manning, P., Niinemets, Ü., Onoda, Y., Ozinga, W.A., Peñuelas, J., Poschlod, P., Reich, P.B., Sandel, B., Schamp, B.S., Sheremetiev, S.N., de Vries, F.T., 2020. Global plant trait relationships extend to the climatic extremes of the tundra biome. Nat. Commun. 11, 1351. https://doi.org/10.1038/s41467-020-15014-4.
Thomson, E.R., Spiegel, M.P., Althuizen, I.H.J., Bass, P., Chen, S., Chmurzynski, A., Halbritter, A.H., Henn, J.J., Jónsdóttir, I.S., Klanderud, K., Li, Y., Maitner, B.S., Michaletz, S.T., Niittynen, P., Roos, R.E., Telford, R.J., Enquist, B.J., Vandvik, V., Macias-Fauria, M., Malhi, Y., 2021. Multiscale mapping of plant functional groups and plant traits in the high Arctic using field spectroscopy, UAV imagery and sentinel-2A data. Environ. Res. Lett. 16, 055006. https://doi.org/10.1088/1748-9326/abf464.
Torabzadeh, H., Morsdorf, F., Schaepman, M.E., 2014. Fusion of imaging spectroscopy and airborne laser scanning data for characterization of forest ecosystems – a review. ISPRS J. Photogramm. Remote Sens. 97, 25–35. https://doi.org/10.1016/j.isprsjprs.2014.08.001.
Turner, W., 2014. Sensing biodiversity. Science 346, 301–302. https://doi.org/10.1126/science.1256014.
Turner, W., Spector, S., Gardiner, N., Fladeland, M., Sterling, E., Steininger, M., 2003. Remote sensing for biodiversity science and conservation. Trends Ecol. Evol. 18, 306–314. https://doi.org/10.1016/S0169-5347(03)00070-3.
Ustin, S.L., Gamon, J.A., 2010. Remote sensing of plant functional types. New Phytol. 186, 795–816. https://doi.org/10.1111/j.1469-8137.2010.03284.x.
Ustin, S.L., Roberts, D.A., Gamon, J.A., Asner, G.P., Green, R.O., 2004. Using imaging spectroscopy to study ecosystem processes and properties. Bioscience 54, 523–534. https://doi.org/10.1641/0006-3568(2004)054[0523:UISTSE]2.0.CO;2.
Van Cleemput, E., Roberts, D.A., Honnay, O., Somers, B., 2019. A novel procedure for measuring functional traits of herbaceous species through field spectroscopy. Methods Ecol. Evol. 10, 1332–1338. https://doi.org/10.1111/2041-210X.13237.
Van Cleemput, E., Adler, P., Suding, K.N., 2023. Making remote sense of biodiversity: What grassland characteristics make spectral diversity a good proxy for taxonomic diversity? Glob. Ecol. Biogeogr. 32 (12), 2177–2188.
Villéger, S., Grenouillet, G., Brosse, S., 2013. Decomposing functional β-diversity reveals that low functional β-diversity is driven by low functional turnover in European fish assemblages. Glob. Ecol. Biogeogr. 22, 671–681. https://doi.org/10.1111/geb.12021.
Walker, M., Humphries, H., Niwot Ridge, L.T.E.R., 2022a. Plant Species Composition Data for Saddle Grid, 1989 - Ongoing. https://doi.org/10.6073/PASTA/EF26A0DBE49EFF4C9F60C1D966F04B94.
Walker, M., Smith, J.G., Humphries, H., Niwot Ridge, L.T.E.R., 2022b. Aboveground Net Primary Productivity Data for Saddle Grid, 1992 - Ongoing. https://doi.org/10.6073/PASTA/B0CDC0CF7C4442F1B2FFC569E9890968.
Wang, R., Gamon, J.A., 2019. Remote sensing of terrestrial plant biodiversity. Remote Sens. Environ. 231, 111218.
Wang, R., Gamon, J.A., Emmerton, C.A., Li, H., Nestola, E., Pastorello, G.Z., Menzer, O., 2016a. Integrated analysis of productivity and biodiversity in a southern Alberta prairie. Remote Sens. (Basel) 8, 214. https://doi.org/10.3390/rs8030214.
Wang, R., Gamon, J.A., Montgomery, R.A., Townsend, P.A., Zygielbaum, A.I., Bitan, K., Tilman, D., Cavender-Bares, J., 2016b. Seasonal variation in the NDVI–species richness relationship in a prairie grassland experiment (Cedar Creek). Remote Sens. (Basel) 8, 128. https://doi.org/10.3390/rs8020128.
Wang, R., Gamon, J.A., Cavender-Bares, J., Townsend, P.A., Zygielbaum, A.I., 2018. The spatial sensitivity of the spectral diversity–biodiversity relationship: an experimental

test in a prairie grassland. Ecol. Appl. 28, 541–556. https://doi.org/10.1002/eap.1669.

Wang, R., Gamon, J.A., Cavender-Bares, J., 2022. Seasonal patterns of spectral diversity at leaf and canopy scales in the Cedar Creek prairie biodiversity experiment. Remote Sens. Environ. 280, 113169. https://doi.org/10.1016/j.rse.2022.113169.

Wang, X., Ye, M., Zhang, X., Xu, R., Xu, D., 2019. Changes in leaf functional traits of Houttuynia cordata in response to soil environmental factors in Anqing city of Anhui Province in China. Environ. Pollut. Bioavailab. 31, 240–251. https://doi.org/10.1080/26395940.2019.1630321.

White, C.T., Morse, J.F., Brandes, H., Chowanski, K., Kittel, T., Losleben, M., Niwot Ridge, L.T.E.R., 2023. Homogenized, Gap-Filled, Air Temperature Data for Saddle, 1986 - Ongoing, Daily. https://doi.org/10.6073/PASTA/D3460079BB2CB633F994A2F4075049EF.

Yang, D., Meng, R., Morrison, B.D., McMahon, A., Hantson, W., Hayes, D.J., Breen, A.L., Salmon, V.G., Serbin, S.P., 2020. A multi-sensor unoccupied aerial system improves characterization of vegetation composition and canopy properties in the arctic tundra. Remote Sens. (Basel) 12, 2638. https://doi.org/10.3390/rs12162638.

Yang, X., Tang, J., Mustard, J.F., Wu, J., Zhao, K., Serbin, S., Lee, J.-E., 2016. Seasonal variability of multiple leaf traits captured by leaf spectroscopy at two temperate deciduous forests. Remote Sens. Environ. 179, 1–12.

Zarco-Tejada, P.J., Miller, J.R., Noland, T.L., Mohammed, G.H., Sampson, P.H., 2001. Scaling-up and model inversion methods with narrowband optical indices for chlorophyll content estimation in closed forest canopies with hyperspectral data. IEEE Trans. Geosci. Remote Sens. 39, 1491–1507.

Zhirin, V.M., Knyazeva, S.V., Eydlina, S.P., 2017. Influence of Forest-canopy morphology and relief on spectral characteristics of taiga forests. Izv. Atmospheric Ocean. Phys. 53, 1019–1028. https://doi.org/10.1134/S0001433817090365.

Zylstra, P., Bradstock, R.A., Bedward, M., Penman, T.D., Doherty, M.D., Weber, R.O., Gill, A.M., Cary, G.J., 2016. Biophysical mechanistic modelling quantifies the effects of plant traits on fire severity: species, not surface fuel loads, determine flame dimensions in eucalypt forests. PloS One 11, e0160715. https://doi.org/10.1371/journal.pone.0160715.